LUND UNIVERSITY

Soil and vegetation-atmosphere exchange of NO, NH_3, and N_2O from field measurements in a semi arid grazed ecosystem in Senegal

Delon, C.; Galy-Lacaux, C.; Serï¿½a, D.; Loubet, B.; Camara, N.; Gardrat, E.; Saneh, I.; Fensholt, R.; Tagesson, T.; Le Dantec, V.; Sambou, B.; Diop, C.; Mougin, E.

LUND UNIVERSITY

PO Box 117
221 00 Lund
+46 46-222 00 00
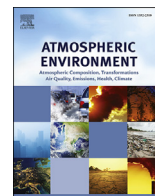
Soil and vegetation-atmosphere exchange of NO, NH₃, and N₂O from field measurements in a semi arid grazed ecosystem in Senegal

C. Delon [a, *], C. Galy-Lacaux [a], D. Serça [a], B. Loubet [b], N. Camara [c], E. Gardrat [a], I. Saneh [d], R. Fensholt [e], T. Tagesson [e], V. Le Dantec [f], B. Sambou [c], C. Diop [c], E. Mougin [g]

[a] Laboratoire d'Aérologie, Université de Toulouse, CNRS, UPS, France
[b] INRA, UMR Ecosys INRA-AgroParisTech, Université Paris-Saclay, Thiverval-Grignon, France
[c] Institut des Sciences de l'Environnement, Université Cheikh Anta Diop, Dakar, Senegal
[d] Centre de Recherche Zootechnique, ISRA, Dahra, Senegal
[e] Department of Geosciences and Natural Resource Management, University of Copenhagen, Denmark
[f] CESBIO, Université de Toulouse, CNRS, UPS, CNES, IRD, Toulouse, France
[g] Geosciences Environnement Toulouse, Université de Toulouse, CNRS, UPS, CNES, IRD, France

HIGHLIGHTS

- At the beginning of the wet season, soil microbial activity is reactivated.
- Significant emissions of NO and CO_2 occur and are linked by microbial processes.
- Litter and straw play an important role in emitting NH_3 and NO (end of wet season).
- NH_3 bidirectional exchange is highlighted and both emission and deposition occur.
- N_2O and NO fluxes are equivalent: denitrification occurs at low soil moisture levels.

ARTICLE INFO

ABSTRACT

The alternating between dry and wet seasons and the consecutive microbial responses to soil water content in semiarid ecosystems has significant consequences on nitrogen exchanges with the atmosphere. Three field campaigns were carried out in a semi arid sahelian rangeland in Dahra (Ferlo, Senegal), two at the beginning of the wet season in July 2012 and July 2013, and the third one in November 2013 at the end of the wet season. The ammonia emission potentials of the soil ranged from 271 to 6628, indicating the soil capacity to emit NH_3. The ammonia compensation point in the soil ranged between 7 and 150 ppb, with soil temperatures between 32 and 37 °C. Ammonia exchange fluctuated between emission and deposition (from $-0.1-1.3$ ng N.m^{-2} s^{-1}), depending on meteorology, ambient NH_3 concentration (5—11 ppb) and compensation point mixing ratios. N_2O fluxes are supposed to be lower than NO fluxes in semi arid ecosystems, but in Dahra N_2O fluxes (5.5 $\pm$ 1.3 ng N m^{-2} s^{-1} in July 2013, and 3.2 $\pm$ 1.7 ng N m^{-2} s^{-1} in November 2013) were similar to NO fluxes (5.7 $\pm$ 3.1 ng N m^{-2} s^{-1} in July 2012, 5.1 $\pm$ 2.1 ng N m^{-2} s^{-1} in July 2013, and 4.0 $\pm$ 2.2 ngN m^{-2} s^{-1} in November 2013). Possible reasons are the influence of soil moisture below the surface (where N_2O is produced) after the beginning of the wet season, the potential aerobic denitrification in microsites, the nitrifier denitrification, and nitrification processes. The presence of litter and standing straw, and their decomposition dominated N compounds emissions in November 2013, whereas emissions in July 2012 and 2013, when the herbaceous strata was sparse, were dominated by microbial processes in the soil. CO_2 respiration fluxes were high in the beginning (107 $\pm$ 26 mg m^{-2} h^{-1} in July 2013) and low in the end of the wet season (32 $\pm$ 5 mg m^{-2} h^{-1} in November 2013), when autotrophic and heterotrophic activity is reduced due to low soil moisture conditions These results confirm that contrasted ecosystem conditions due to drastic changes in water availability in semi arid regions have important non linear impacts on the biogeochemical nitrogen cycle.

* Corresponding author.
E-mail address: claire.delon@aero.obs-mip.fr (C. Delon).

1. Introduction

Nitrous oxides (N$_2$O), nitrogen monoxide (NO) and ammonia (NH$_3$) play important roles in the atmosphere, from the local up to the global scale (Hertel et al., 2011). Nitrous oxide is a powerful greenhouse gas which also contributes to the destruction of stratospheric ozone (Butterbach-Bahl et al., 2013). Nitrogen monoxide (NO) contributes to the formation of tropospheric ozone and modifies the oxidative capacity of the atmosphere (Steinkamp et al., 2009). In non-urbanized areas, where anthropogenic emissions are negligible, the soil emission of biogenic NO plays an essential role in regional atmospheric chemistry (Pilegaard, 2013). Ammonia (NH$_3$) is mainly emitted by agricultural activities, and also by the decomposition of litter and volatilization of animal excreta (Sutton et al., 2009; Massad et al., 2010). It is an essential precursor of Secondary Organic Aerosol (SOA). (Fuzzi et al., 2015). To quantify and understand these impacts of reactive and greenhouse gases on tropospheric chemistry, it is of prime importance to understand the processes leading to emissions and exchanges of these compounds, as well as the parameters affecting them. Indeed, fluxes of gaseous N compounds between biosphere and atmosphere are closely coupled to the biogeochemical processes within the vegetation and the soil. Carbon, nutrients and water cycling, as well as anthropogenic and animal pressure are also key issues for interpreting these fluxes in time or space (Arneth et al., 2012).

The particular context of semi arid regions (such as the Sahel) involves specific conditions: the Sahel is mainly covered by semi arid grasslands, with shrubs and low tree density. Semi arid grasslands have been identified as important sources of nitrogen compounds at the global scale (Hudman et al., 2012), even though soils are known to hold limited amounts of nutrients (C, N). Despite this low N supply, N cycling is rapid in semi arid and arid lands: decomposition is fast and driven by an abundant micro fauna that contributes to a fast N turnover. This rapid turnover in semi arid and arid soils leads to low nutrient accumulation (Schlesinger et al., 1990). Another factor affecting the N availability is the presence of livestock which increases the N availability in these ecosystems. Grazers have multiple effects on the N cycle in the soil, and on N availability to plants, via urine, dung and trampling (Frank and Evans, 1997; Rufino et al., 2014).

Specific climatic conditions have to be taken into account in the Sahel: at the beginning of the rainy season, the soil moisture becomes sufficient to activate the microbial activity in the soil (Bouwman et al., 2002; Meixner and Yang, 2006), NO and N$_2$O (and CO$_2$) emissions are larger than in the dry season, and large bursts of emission are produced when first precipitations shower long-dried soils (Yienger and Levy, 1995; Jaeglé et al., 2004, Delon et al., 2008, 2015; Hudman et al., 2010; Delon et al., 2015; Elberling et al., 2003).

NO and N$_2$O emissions are controlled by nitrification and denitrification processes, driven by the underlying microorganism population producing and consuming NO and N$_2$O in the soils, depending on biotic and abiotic processes (Meixner and Yang, 2006; Butterbach-Bahl et al., 2013). Soil moisture is a major regulator of these emissions as it affects the oxygen availability to soil microbes. NO and N$_2$O emissions are also regulated by substrate concentration, plant nitrate uptake, litter/soil organic matter quality, root/microbial respiration, soil texture and temperature, predation, pH, wind speed, N input (Chapin et al., 2002; Delon et al., 2007; Pilegaard, 2013).

N$_2$O, NO and soil respiration are considered as one way only, even if NO and N$_2$O deposition exists in very specific conditions (Grote et al., 2009), measurements did not show deposition in this study. Biosphere-atmosphere exchange of NH$_3$ is bi-directional and the net flux is the combination of different exchange pathways between the plant (cuticle and stomata), the soil, the leaf litter and the atmosphere. The overall NH$_3$ flux for a given surface may switch from net emission to net deposition at sub-hourly, diurnal and seasonal scales (Sutton et al., 2009; Massad et al., 2010; Loubet et al., 2012). NH$_3$ can rapidly be deposited onto cuticles due to its high solubility. The so called canopy compensation point is a powerful concept to study NH$_3$ exchange. It expresses the atmospheric NH$_3$ concentration for which the flux between the surface and the atmosphere switches from emission to deposition, or *vice versa* (Farquhar et al., 1980), and it depends on the emission potential, defined as the [NH$_4^+$]/[H$^+$] ratio at the soil and leaf level, thee pH being a major chemical control of the fluxes (Flechard et al., 2013). The direction and magnitude of NH$_3$ exchanges depend on the NH$_3$ concentration difference between the canopy and the atmosphere, and on a large range of environmental factors including meteorology (particularly air humidity, which will influence surface wetness), vegetal cover and soil characteristics. NH$_3$ emissions are also strongly sensitive to soil moisture conditions, and relationships between NO and NH$_3$ soil fluxes have been identified through the ammonium content in the soil (McCalley and Sparks, 2008).

Emissions of N$_2$O, NO from bare soils and litter have, as far as the authors know, rarely been quantified by direct measurements over tropical semi arid regions, (*e.g.* Serça et al. (1998), Le Roux et al. (1995) for NO, Grote et al. (2009) for N$_2$O and CO$_2$), mainly because experimental conditions are difficult (no power supply, very hot temperatures, remote sites of study) and also because most measurements techniques, such as micrometeorological techniques, imply expensive and complex devices. The number of studies of NH$_3$ exchange over semi natural land is rather limited (Wichink Kruit et al., 2007; Wentworth et al., 2014) but some work has been done in temperate ecosystems (Flechard and Fowler, 1998a,b; Flechard et al., 1999, 2013; Loubet et al., 2012). Semi-natural vegetation is defined as vegetation not planted by humans but influenced by human actions (FAO and LCCS, 2000). However, such studies are still missing for tropical and semi arid ecosystems, where, as mentioned before, the quantification of exchange fluxes between the soil and the atmosphere is challenging.

The objectives of this study are i) to explore surface atmosphere exchanges of NO, N$_2$O, and NH$_3$ and their link with microbial processes in the soil (leading as well to soil respiration and CO$_2$ emissions), in a semi-arid region in contrasting ecosystem conditions at the beginning and end of the wet season (different soil humidity and vegetation cover), ii) to investigate the emissions from litter at the end of the rain season, iii) to quantify N compound emissions in semi arid soils.

To reach these objectives, we have applied chamber techniques for measuring NH$_3$, NO, CO$_2$ (dynamic chamber) and N$_2$O (static) fluxes. These techniques have the major advantage of being robust and of reduced costs, and have been widely used and validated in many studies (Davidson, 1991, Gut et al., 2002; Pape et al., 2009, Laville et al., 2011; Tagesson et al., 2012; Almand-Hunter et al., 2015 and references therein). After presenting the field site, the chamber techniques and the calculations of fluxes for each compound, processes of emission and exchanges are investigated. Measurements of meteorological and edaphic conditions are used to understand the variability in NO, N$_2$O, NH$_3$ and CO$_2$ fluxes at the Dahra site (Senegal, Ferlo).

2. Materials and methods

2.1. Field site

The Dahra field site is located in Senegal (Ferlo), West Africa (15°24′10″N, 15°25′56″W, elevation 40 m, Fig. 1a). This site is a semi-arid savanna, primarily used as grazed rangeland (Tagesson
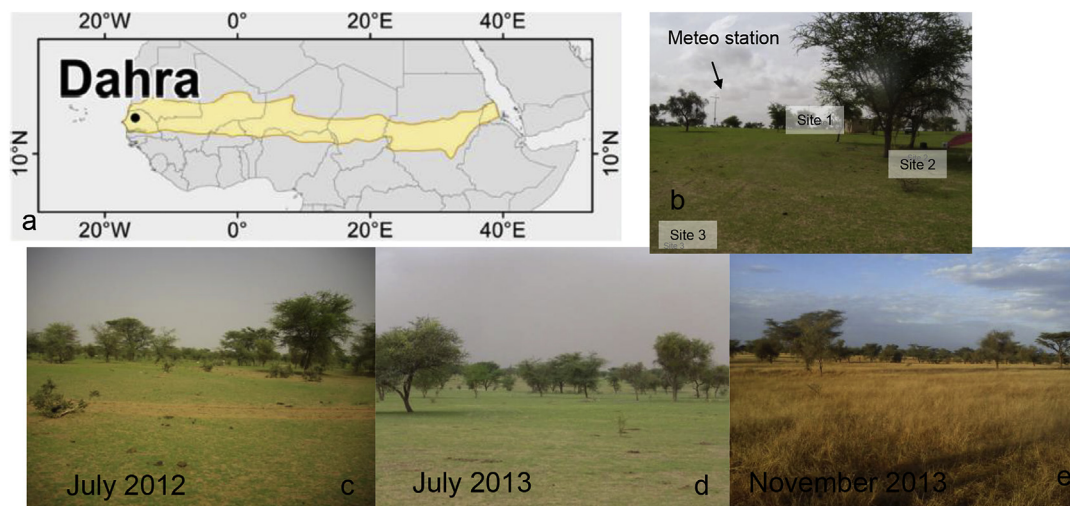
Fig. 1. (a) localisation of the Dahra site in West Africa. (b) spatial distribution of the three sites of measurements at the Dahra site. (c) Dahra site in July 2012, (d) Dahra site in July 2013, (e) Dahra site in November 2013.

et al., 2015b). The rainy season occurs from July to October approximately (3—4 months). The tree coverage is low, about 3% (Rasmussen et al., 2011). The most abundant tree species are the *Balanites aegyptiaca, Acacia tortilis* and *Acacia Senegal*. The herbaceous vegetation is dominated by annual C4 grasses (*e.g. Dactyloctenium aegyptium, Aristida adscensionis, Cenchrus biflorus* and *Eragrostis tremula*) (Tagesson et al., 2015b). The livestock consists mainly of cows (*Bos taurus indicus*), sheep (*Ovis aries*), and goats (*Capra aegagrus hircus*) and grazing is permanent and occurs year-round. The Dahra field site is located within the 'Centre de Recherche Zootechnique (CRZ)' managed by the Institut Sénégalais de Recherche Agronomique (ISRA). Ground photographs of the Dahra site in July 2012, July 2013 (short vegetation, beginning of growing period) and November 2013 (high standing straw, end of wet season) are shown in Fig. 1c,d,e. At Dahra, the soil is sandy, with 89% of sand and 6.3% of clay (the rest being silt) for the 0—5 cm horizon. Surface pH ranges from 6.16 to 7.43, depending on the place where the measure is done. Mean meteorological and soil characteristics of the study site are reported in Table 1.

This study is based on measurements performed during three field campaigns which lasted 7 days in July 2012 (11—17 July 2012), 8 days in July 2013 (11—18 July 2013) and 10 days in November 2013 (29 October-7 November 2013).

2.1.1. Sampling sites

The samples were taken at three different locations (top, middle and bottom) along a 500 m transect following a dune slope (Fig. 1b, sites 1, 2, 3), with one location per day. Each location was then sampled every 3 days, from 8 a.m. to 7 p.m. approximately for soil

fluxes, and 24 h a day for concentrations. Top site was sampled respectively 2, 3 and 4 times in J12, J13 and N13, middle site was sampled respectively 2, 3 and 3 times in J12, J13 and N13, and bottom site was sampled respectively 2, 2 and 3 times in J12, J13 and N13. The herbaceous vegetation cover is rather homogeneous in the field, ensuring that the plot of soil cover inside the chamber is representative of the area (Fensholt and Sandholt, 2005; Fensholt et al., 2006).

2.1.2. Watering experiments

In order to check for a dependence of NH_3 and NO flux with soil moisture, we simulated a 20 mm rainfall event on 15 July 2013 and 4 November 2013. Flux measurements were performed on 16, 17 (first flux measured 24 h after watering) and 18 July, 4 November (first flux 4—7 h after watering) and 7 November. 28 fluxes were measured in July, and 14 in November. These measurements are specifically analyzed for each gas and are not mixed with fluxes measured in non watered plots. Soil moistures in the watered plots are 10% 16 July, 8% 17 July, 5% 18 July, 17% 4 November, 7% 7 November. As for non watered plots, the samples were taken at top, middle, and bottom slope of the dune transect and only daily averages are presented.

2.2. NO and NH_3 chamber flux measurements

NH_3 and NO exchange fluxes were measured with manual closed dynamic chambers (non-steady-state through-flow chambers as defined in Pumpanen et al. (2004)). This technique has already been used by Akiyama et al. (2004), Roelle &Aneja (2002),

Table 1
Main characteristics of the Dahra site in 2012 and 2013. (a) averages from 13 samples.

Field name	Dahra
Location	15°24′10″N, 15°25′56″W
Elevation	40 m
Mean annual precipitation	514 mm in 2012, 355 mm in 2013
Mean annual temperature	28 °C in 2012, 29 °C in 2013
Soil type	sandy
Dominant tree species	*Balanites aegyptiaca, Acacia tortilis* and *Acacia senegal*
Dominant ground vegetation	*Dactyloctenium aegyptium, Aristida adscensionis, Cenchrus biflorus* and *Eragrostis tremula*
Sand percentage (a)	89% (86—92)
Clay percentage (a)	6.3% (4.5—7.9)

Zhang et al. (2011) for NH$_3$ fluxes above fertilized soils. More details about the fluxes calculation can be found further.

2.2.1. NO/NO$_2$/NH$_3$ analyzer

A Thermoscientific 17C (ThermoFischer Scientific, MA, USA) was used in July 2012 for NO/NO$_2$/NH$_3$ concentration measurements, while in July and November 2013 we used a Thermoscientific 17i ((ThermoFischer Scientific, MA, USA, Fig. 2a). These analyzers use a chemoluminescence detector for NO. The air sample enters the reaction chamber and reacts with the O$_3$ generated by an internal generator. This reaction produces a luminescent radiation directly proportional to the NO concentration. The air sample is sequentially drawn through a molybdenum converter heated to 325 °C which converts a fraction of NO$_2$ to NO, and a stainless steal converter heated to 750 °C which converts a fraction of NH$_3$ and NO$_2$ to NO. The detector hence measures rNO, then r(NO + αNO$_2$), and finally r(NO + βNO$_2$ + γNH$_3$), where r is the NO detection efficiency, α and β are the NO$_2$ conversion efficiency of the molybdenum and stainless steel converters and γ is the NH$_3$ conversion efficiency of the stainless steel converter. The efficiencies are determined by the calibration procedure and NO, NO$_2$ and NH$_3$ concentrations are deduced by manipulating the three expressions. The converters also convert other nitrogen compounds. Especially the molybdenum converter is known to convert Peroxyacetyl nitrate (PAN), nitrous acid (HONO), nitric acid (HNO$_3$) and organic nitrates (Parrish and Fehsenfeld, 2000; Dari-Salisburgo et al., 2009). These interferences have generally lower concentrations than NO$_2$, and in those conditions valid NO$_2$ concentrations may be obtained (Dunlea et al., 2007). The 17i instrument is a more recent version than the 17C instrument, and both these analyzers have been widely used for NH$_3$ concentrations and/or fluxes measurements (Roelle and Aneja., 2002; Zhang et al., 2011; Ni et al., 2000; Phillips et al., 2004; Akiyama et al., 2004).

Calibrations of the analyzer were done before and after each field campaign with a reference NO/NOx/air mixture at 205 ppbv ± 3.2 ppbv (COFRAC certified). Two other points were generated at 100 and 800 ppbv to ensure the linearity of the response. The standard gas used for NO is NF EN14211. In addition, the analyzer was calibrated using a bottle of NH$_3$ (concentration 2 ppm) without dilution (pure gas). The lower detection limit was 1 ppbv, the precision ± 0.4 ppbv (for a 500 ppbv range), and the averaging time 10s. The response time of the analyzer was 120s, *i.e.* 90% of the actual concentration is reached after 120s.

The time needed for the sample to reach the reaction chamber, calculated using the volume of the Teflon PFA tubing (length 4 m and internal diameter 0.0044 m) and the pump flow (0.6l min^{-1}), was 6s.

2.2.2. Dynamic chambers

A measurement system was developed in this study and includes a portable opaque Teflon chamber (Fig. 2b) and the NO/NO$_2$/NH$_3$ analyzer described above. All of the system was power supplied by a power generator, located 100 m away in the field. To avoid NH$_3$ deposition onto water or stainless steel, neither frame nor seals were used during the measurements. The chamber was inserted approximately 2 cm directly into the sandy soil to avoid air leakages. The external volume of the chamber was 40 cm × 20 cm × 20 cm. The useful volume was 18 × 38 × 18 cm^3 (12.3l or 0.0123 m^3), due to the thickness of the Teflon walls. The air inlet is on one side of the chamber (a small vent of 4 mm in diameter provided the pressure equilibrium between the inside and outside of the chamber). The air outlet on the other side is connected to the analyzer with a 4 m Teflon tube. The chamber is continuously swept with an air flow Q of 0.6 L min^{-1} (or 10^{-5} m^3 s^{-1}) insured by the instrument pump, and the air flow is controlled inside the analyzer by a flow meter. The air residence time in the chamber is approximately 20 min (Volume/flow), and the chamber is maintained in place for 10 min. Inside the chamber, the opaque walls minimize photochemical reactions which are considered as negligible. After 10 min, the chamber is turned over in order for the analyzer to be swept by ambient air. After 5 min of ambient air concentration measurement, the chamber is placed again on the soil to begin a new cycle.

The calculation of fluxes are based on the closed dynamic chamber technique, with the following assumptions: the concentration in the chamber is equal to the concentration leaving the chamber to the analyzer, no deposition occurs onto the Teflon walls chamber; chemical reactions in the gas phase inside the chamber
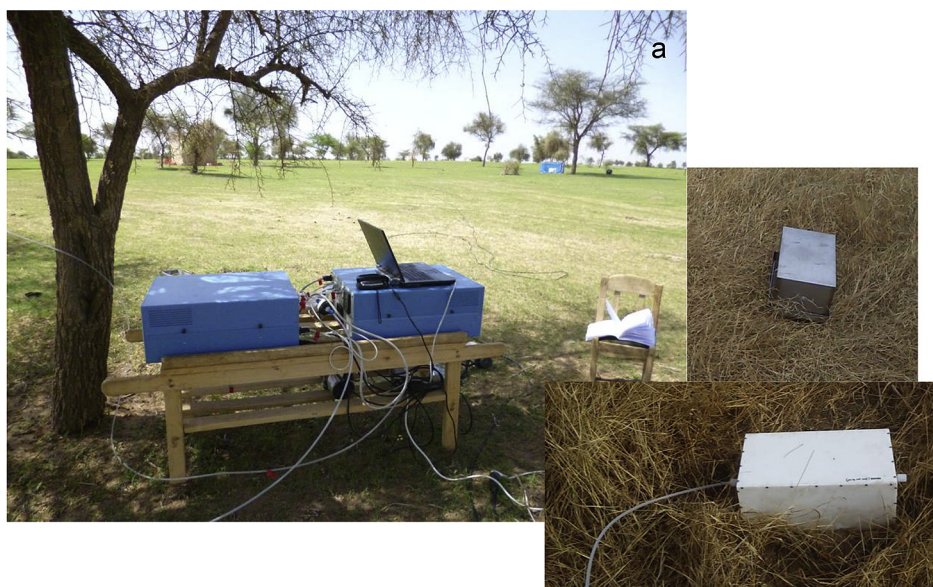

Fig. 2. Sampling device for N compound flux measurements. (a) ThermoScientifics © 17i for NO/NO$_2$/NH$_3$ concentrations, (b) Teflon chamber for NO & NH$_3$ flux measurements, (c) Stainless steal chamber for N$_2$O flux measurements.

are limited thanks to opaque walls; the air flow rate Q (m³ s⁻¹) is constant and ensures that the mass of gas (NH₃ or NO) within the chamber at time $t + \delta t$ equals to the mass of gas present at time t plus (if emission) or minus (if deposition) the mass of gas entering the chamber in the δt interval (soil flux), minus the mass of gas leaving the chamber to the analyzer in the same δt interval. Assuming the gas entering the chamber has a concentration C_{out} (mol m⁻³), and that neither chemical reaction nor wall deposition occurs, the mass balance equation in the chamber can be simplified to:

$$V \frac{\partial C_X}{\partial t} = (F_X A_0 - Q C_X + Q C_{out}) \tag{1}$$

Where F_X is the flux (NH₃ or NO) in nmol m⁻² s⁻¹, C_X is the concentration in the chamber outlet in mol m⁻³. $A_0 = 0.0684$ m² is the surface of the ground covered by the chamber, $V = 0.0123$ m⁻³ is the volume of the chamber, $R = 8.2 \times 10^{-5}$ m³ atm K⁻¹ mole⁻¹ is the gas constant, and T (K) is the air temperature in the chamber. NH₃ and NO concentrations are recorded every 10 s, with a Lab-View© application. $\partial C_X / \partial t$ is the initial rate of increase in NH₃ or NO mixing ratios calculated by linear regression, t is in seconds. Equation (1) can be integrated which yields:

$$C_X(t) - C_{out} = \frac{F_X A_0}{Q} \left[1 - \exp\left(-\frac{Q}{V} t \right) \right] \tag{2}$$

$$F_X = \frac{Q}{A_0} [C_X(t) - C_{out}] \times \left[1 - \exp\left(-\frac{Q}{V} t \right) \right]^{-1} \tag{3}$$

If the dilution due to outside air can be considered small, which happens when the term $\frac{Q}{V} t$ is small, hence when the time t is small, then the exponential term can be reduced to its limited development $1 - \frac{Q}{V} t$ which yields for the flux:

$$F_X = \frac{V}{A_0} \frac{[C_X(t) - C_{out}]}{t} = \frac{V}{A_0} \frac{\delta C_X}{\delta t} \tag{4}$$

We get a similar expression as in Davidson, (1991), which is true shortly after the chamber was closed (time $t = \delta t$, and concentration increased by δC_X relative to outside air). A linear regression was calculated during the first 120s for NH₃, and 180–300s for NO, following the installation of the chamber on the soil. A lag time of 20s was removed to account for the air being transported through the Teflon tubing (10s) and for the analyzer response time (10s). This 120s time (180–300s) for NH₃ (for NO) has been chosen because the increase in ammonia (NO) concentration showed a maximum slope value during this interval. The dilution effect due to mixing of outside air in the chamber was evaluated based on our set up in which $Q/V = 8.13 \times 10^{-4}$ s⁻¹. As a consequence, the NH₃ concentration needs a 5% correction after 120s and the NO concentration needs a 7%–11% after 180–300 s. Fx is further converted in ngN m⁻² s⁻¹.

Considering the precision of the analyzer (±0.4 ppbv), the minimum flux detected by this device would be 0.3 ngN m⁻² s⁻¹ for NH₃ and 0.2 ngN m⁻² s⁻¹ for NO.

For NO, fast gas phase reactions NO + O₃ → NO₂ have to be considered in the calculation of each individual chamber flux. This necessitates the simultaneous measurement of all three trace gases, which was not done in our field campaigns. However, the underestimation due to photochemistry can be approached with the median NO concentration sampled before flux measurements (2.19 ppb in J12, 2.05 ppb in J13, 1.11 ppb in N13), and with the climatological ozone mixing ratio taken from Adon et al. (2010) in comparable dry savanna ecosystems (18 ppb in July, 9 ppb in November). Following Pape et al. (2000) and Delon et al. (2015), the

underestimation of NO fluxes is calculated from the relation k.[NO]·[O3] where k is the reaction rate constant. The underestimation is 47% in J12, 48% in J13 and 10% in N13, taking into account mean air temperature given in Fig. 3 for the reaction rate constant estimation (Pape et al., 2000). The uncertainty on the resulting flux is mostly influenced by the lack of ozone concentration measurements, and is not distinguishable from the estimation of the correction due to photochemistry.

In the following results, the NO and NH₃ fluxes are recalculated according to these underestimation.

2.2.3. Data quality check

Not all the NH₃ fluxes were kept after quality checking of the calculated ammonia fluxes, based on two criteria.

- The coefficient of determination R^2 estimated from the linear regression of the increase in the gas concentration in 120s had to be higher than 0.4 (considered as a weak but existing and significant correlation).
- The concentration difference between last and first measurement points had to be superior to 0.4 ppb (sensitivity of the analyzer). Actually, for concentration differences below 0.4, R^2 were also lower than 0.4.

Finally, 122/140 fluxes (87%) satisfied these criteria in July 2012, 116/134 (86%) in July 2013 and 157/191 (82%) in November 2013 for NH₃ flux measurements. All NO flux measurements and all NH₃ fluxes from watered plots fulfilled these criteria and none were filtered out.

As the NH₃ flux is calculated for a 120s time interval, and considering that 90% of the real concentration is reached after this time, this calculation within a 120s time interval underestimates the flux on the order of 9% (i.e. the real concentration difference is 9% greater than the measured concentration difference). Other uncertainties were not quantified, such as deposition of ammonia inside the 17C/17i analyzer and during the transfer between soil chamber and analyzer. Further NH₃ fluxes are recalculated according to this 9% underestimation.

2.3. N₂O chamber flux measurements

N₂O fluxes were measured using the static chamber (non-flow-through non-steady state) method. One stainless steel chamber with a base of 0.20 m × 0.40 m and with a height of 0.15 m was placed on a frame (previously inserted 3 cm in the soil) and sealed by a slot filled with water (Fig. 2c). The N₂O chamber was placed approximately 1 m close to the Teflon chamber used for NO and NH₃ flux measurements. N₂O fluxes were sampled at least 3 times a day.

Samples of the chamber headspace gas were removed with a syringe through a rubber septum at time 0, 15, 30 and 45 min after placing the chamber on the frame. Air samples were injected from the syringe to 10-ml glass vials which contained 6M NaCl solution capped with high density butyl stoppers and aluminum seals. When injected, the air sample chases away almost all the solution from the vials (a small quantity is kept inside), and the vials are kept upside down to ensure air tightness. All samples were subsequently analyzed by gas chromatography in the lab two to three weeks after the field campaign. Analysis of N₂O concentrations were performed by Gas Chromatography (GC) on a SRI 8610C gas chromatograph (SRI, Torrance, CA, USA) equipped with an electron capture detector (ECD). Simultaneous integration of peaks is made using the Peak Simple 3.54 software (SRI, Torrance, CA, USA). Gas standards (347 and 1020 ppbv for N2O Air Liquid "crystal" standards, uncertainties less than 10%) were injected after every 10 samples of analysis to

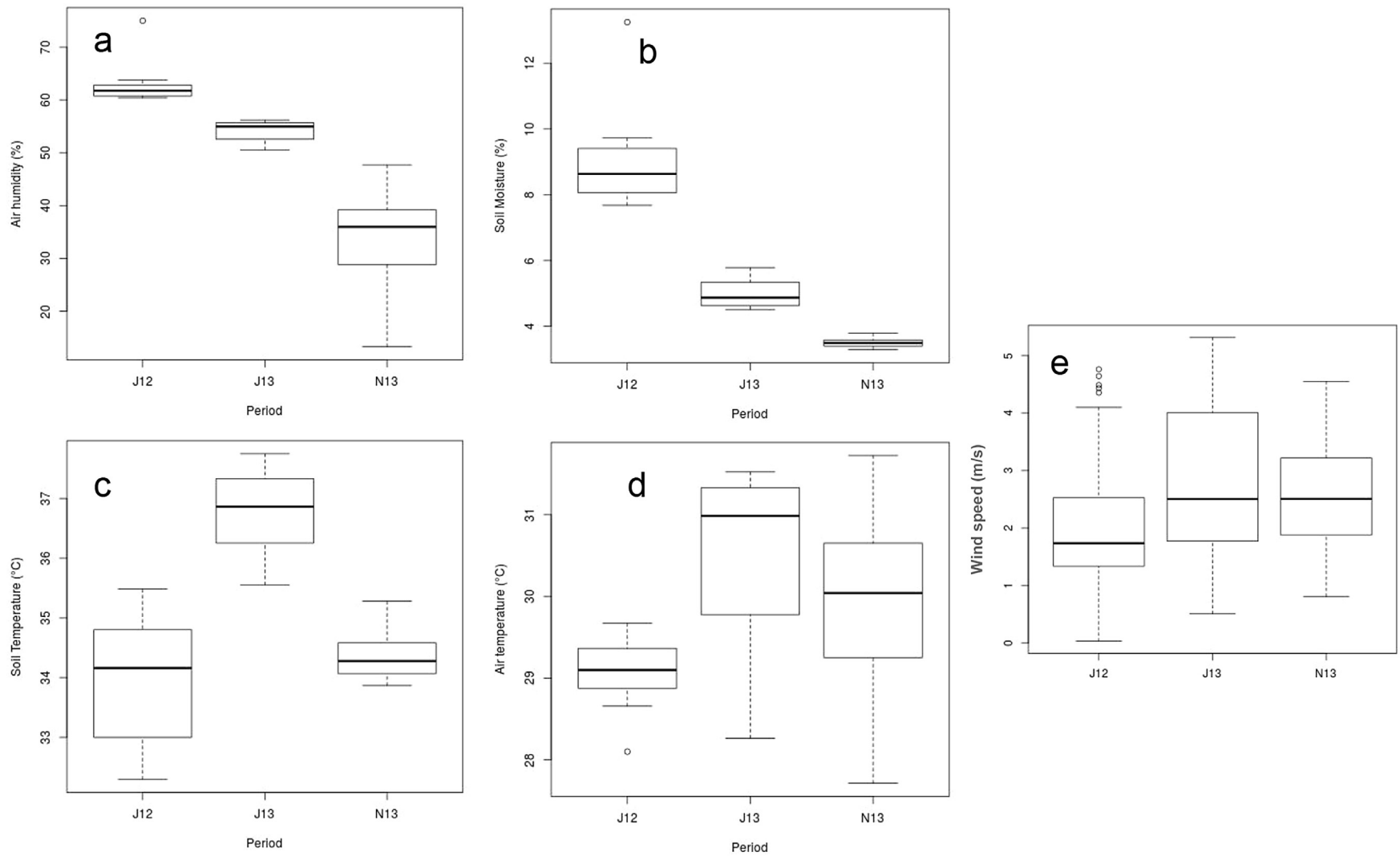**Fig. 3.** Boxplots of mean meteorological parameters values during the three campaigns. J12: July 2012, J13: July 2013, N13: November 2013. (a) Air humidity in %, (b) Soil moisture in % (c) Soil temperature in °C (d) Air temperature in °C (e) Wind speed in m/s. Thick line is the median, upper (lower) line of the box is the 75% (25%) quartile and dotted line is 1.5 times the interquartile distance.

calibrate the GC. Duplicate injection of samples showed reproducibility better than 5%.

N$_2$O fluxes were calculated from the slope of the linear regression of gas concentration in the chamber versus time, as for NO and NH$_3$ fluxes, and as done in several studies on N$_2$O flux measurements (e.g. Assouma et al., 2016; Butterbach-Bahl et al., 2004; Livesley et al., 2011, Marquina et el., 2013; Predotova et al., 2010) The coefficient of determination R^2 estimated from the linear regression had to be higher than 0.5. Considering the precision of the analysis (2–4 ppbv), the minimum flux detected by this device would be 0.07 to 0.14 ngN m^{-2} s^{-1}. 93% and 87% of the fluxes were kept after applying these criteria in J13 and N13 respectively. No correction was applied due to chemistry or dilution.

2.4. Soil respiration (CO$_2$ emission) measurements

CO$_2$ fluxes were measured using a manual closed dynamic chamber (SRC-1 from PP-systems, 150 mm height x 100 mm diameter) coupled to a non-dispersive infrared CO$_2$/H$_2$O analyzer EGM-4 (PP-Systems, Amesbury, MA 01913, USA). Using infra-red gas analysis techniques, instantaneous measurements are performed with accuracy lower than 1% of span concentration. The respiration is measured by placing the closed chamber on the bare soil and measuring the rate of increase of the CO$_2$ concentration inside the chamber during 120 s maximum (Le Dantec et al., 1999; Ngao et al., 2006). Then, assuming a well mixed sealed system:

$$R = \frac{C_n - C_0}{T_n} \times \frac{V}{A} \qquad (5)$$

Where R is the respiration rate (Flux of CO$_2$/unit area/unit time), Co is the CO$_2$ concentration at T = 0 and Cn is the concentration at a time Tn later, A is the area of soil exposed and V the total system volume. The quality control is made by the PP-SYSTEMS. This control consists in checking the linearity of the rate of increase in CO$_2$ once the chamber has been placed on the soil. If the increase in CO$_2$ concentration with time (concentration measured every 8 s) is non-linear, a warning is given by the system.

2.5. Meteorological station

The measured meteorological variables were rainfall (mm), air temperature (°C), and relative air humidity (%) at 2 m height, soil surface temperature (°C), and soil surface moisture (%) at 0.05 m depth. Data were sampled every 30 s and stored as 15 min averages (sum for rainfall). Sensor information and details on all measured variables are available in Tagesson et al. (2015b).

2.6. Soil characteristics (texture, pH, N content)

During the three field campaigns, additional measurements were carried out to address some biogeochemical characteristics of the site. Soil samples (0–5 cm) were taken from each location where the measurements were done (top, middle and bottom slope). Samples were dried in ambient conditions (mean daily temperature is approximately 35 °C), and stored in the dark for determination of texture, ammonium (NH$_4^+$) concentrations, C/N ratio, total C, total N, and pH at the Laboratoire d'Analyses des Sols d'Arras (http://www5.lille.inra.fr/las, NF EN ISO/CEI 17025: 2005) in July 2012 and July 2013, and at the GALYS Laboratoire (http://www.galys-laboratoire.fr/, NF EN ISO/CEI 17025: 2005) in November 2013. The analyses were performed within a 4 week period after sampling. One may hypothesize that ammonium content in litter or in soils has not been changed due to volatilization or chemical transformation during transport and storage

thanks to the very low soil moisture level in samples. Indeed, microbial activity and mineralization processes are inhibited in low soil moisture conditions, even when soil temperature is high (Bai et al., 2013, and references therein).

Soil texture is determined according to norm NF X 31–107. Clay (<2 µm), thin silt (2 µm–20 µm), coarse silt (20 µm–50 µm), thin sand (0,050 mm–0,200 mm), coarse sand (0,200 mm–2,00 mm) are determined without decarbonatation. Organic carbon and total nitrogen are determined following norm NF ISO 10694. The whole carbon of the sample is transformed into CO$_2$. The CO$_2$ is therefore measured by thermal conductibility. Mineral and organic nitrogen are determined following norm NF ISO 13878. The sample is heated at 1000 °C with O$_2$. Products of combustion or decomposition are reduced in N$_2$. N$_2$ is therefore measured by thermal conductibility (catharometer). pH is determined with norm NF ISO 10390, with. soil samples stired with water (ratio 1/5).

2.7. Soil ammonia emission potential Γ and compensation point

Measurements of soil pH and NH$_4^+$concentrations yielded to the quantification of soil emission potentials at the Dahra site. The soil emission potential Γ is the ratio of [NH$_4^+$] to [H$^+$] concentrations in the water solution of the soil (mol.L^{-1}). A large Γ indicates that the soil has a high propensity to emit NH$_3$, considering that the potential emission of NH$_3$ depends on the availability of ammonium in the soil and on the pH. The soil compensation point χ$_g$ has been calculated from the emission potential Γ, as a function of soil surface temperature Tg (Nemitz et al., 2001):

$$\chi_g = \frac{161500}{T_g} \exp\left(\frac{-10378}{T_g}\right) \times \Gamma \quad \text{with} \quad \Gamma = \frac{\left[NH_4^+\right]}{\left[H^+\right]} \qquad (6)$$

2.8. Stepwise multiple regression analysis

A stepwise linear multiple regression analysis was performed between daily averaged gas fluxes (NO, NH$_3$, N$_2$O, CO$_2$) and relevant available daily averaged parameters such as soil moisture and temperature at 5 cm depth, air humidity and temperature, wind speed and ambient NH$_3$ concentration (used only to explain NH$_3$ fluxes). Soil parameters such as mineral nitrogen, total N and organic C, soil texture and pH could not be used unfortunately in the same data base since their relative measurements did not have the same temporal resolution as the other parameters.

The R software (http://www.R-project.org) was used to provide results of this linear regression analysis.

3. Results and discussion

3.1. Meteorological data

Fig. 3 shows mean relative air humidity, soil moisture, soil temperature, air temperature and wind speed calculated for each field campaign (J12 = July 2012, J13 = July 2013, N13 = November 2013). Soil moisture is higher in J12 (mean is 9.2%) because a rain event occurred the day before the beginning of the campaign on 9/7/2012. A second rain event occurred at the end of the campaign (16/7/2012). Mean soil moistures are respectively 5% and 3.5% in J13 and N13. Soil moistures are significantly different between the three periods (p < 0.05). Air and soil temperatures are lower in J12 (means are respectively 29 and 34 °C) than in J13 (30 and 37 °C) because of these rain events. In N13, the presence of straw prevents the soil from strong heating (mean air and soil temperatures are

respectively 30 and 34 °C). The lower difference between air and soil temperatures is therefore found in N13 (4 °C, *vs.* 5 °C and 7 °C in J12 and J13). Soil temperatures are significantly different between J12 and J13, and between J13 and N13 (p < 0.05), but not between J12 and N13. Daily rainfall measurements are reported in Fig. 4, as well as periods of field campaigns.

3.2. Total nitrogen and ammonium content

Table 2 gives the averages of soil characteristics in Dahra based on the entire range of values for each campaign. Soil Organic Carbon (SOC) and Total N are respectively 4.7 ± 1.3 g/kg and 0.36 ± 0.10 g/kg in J12, 5.0 ± 0.7 g/kg and 0.39 ± 0.05 g/kg in J13, 4.7 ± 1.3 g/kg and 0.42 ± 0.13 g/kg in N13. Table 3 provides individual values for pH, $[NH_4^+]$, Γ_g and χ_g, when pH and $[NH_4^+]$ measurements were performed. $[NH_4^+]$ values measured in Dahra at two different seasons are equivalent to values found in the Fakara region (Niger Sahel, Turner and Hiernaux, 2015), *i.e.* 2.71 ± 2.34 mg/kg collected at the end of the dry season in 2008, whereas total N content are lower in the Fakara (0.15 ± 0.06 g/kg). Mean $[NH_4^+]$ are 3.4 ± 3.4 mg/kg in J12, and 1.6 ± 1.1 mg/kg in N13. Since no $[NH_4^+]$ is available in J13, we have calculated a value from J12 data, and found that $[NH_4^+]$ represents around 0.6% of total Nitrogen, or a mean $[NH_4^+]$ equal to 2.3 ± 0.3 mg/kg when applied in J13.

3.3. Soil emission potential Γ_g and compensation point χ_g

Considering the values in Table 3, the mean soil emission potential for the three campaigns would be 1300 ± 1700, with values

ranging from 254 to 6628. In July 2012, the highest values are linked to soil samples collected after the rain event which occurred on 9 July. Afterwards, soil samples show a sharp decrease in ammonium concentrations (Table 3). A mean emission potential, calculated without the extreme values of July 11 and 12 July, would be more representative of a mean state, and would be around 400 (±100) for J12 campaign. In J13, an emission potential around 500 is found. In November 2013, the average soil emission potential is 2385 ± 1387, because of a higher soil pH. Higher pH after the rain season could be explained by the strong alkaline characteristics of precipitation, due to high loading of particulate matter in the atmosphere common to semi-arid region conditions. Dust is rich in calcium bicarbonate/carbonate representing a major buffering agent for acidity generated by sulphuric, nitric and organic acids (Laouali et al., 2012; Galy-Lacaux and Modi, 1998).

Considering the Massad et al. (2010) review, Γ values in non-fertilized soils are significantly lower than in fertilized soils. This is mainly due to lower ammonium content in the former ecosystems. Soil emission potential values depend strongly on land-use

Table 2
Soil characteristics and ammonia concentrations (at 1.5 m) averaged for each field campaign. Numbers in parenthesis give the number of samples used for averages except for [NH₃] which is measured continuously.

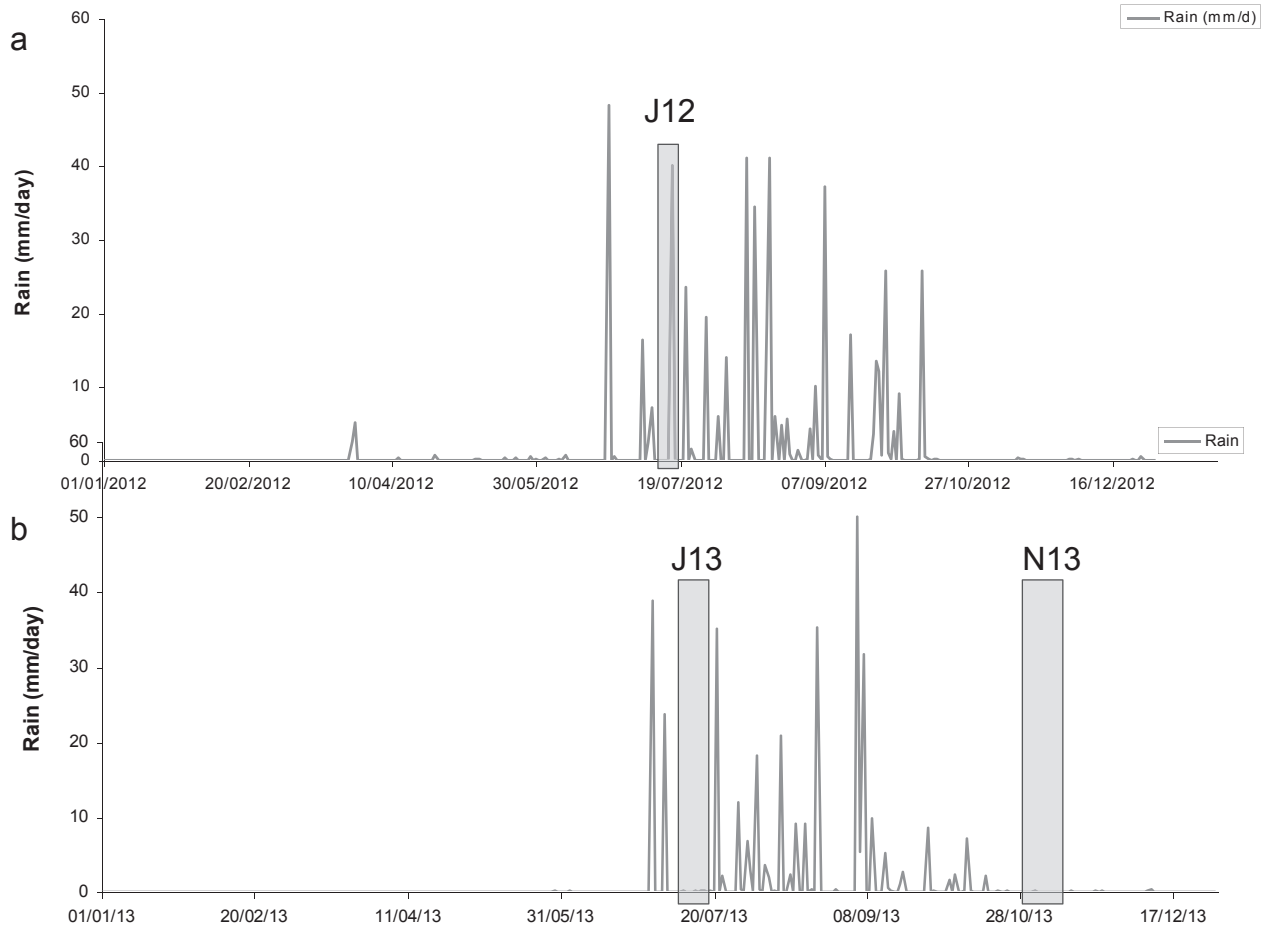| Period	C/N ratio	Total C (g/kg)	Total N (g/kg)	[NH₃] (ppb)
J12 (10)	13.1 ± 0.6	4.7 ± 1.3	0.36 ± 0.10	8.8 ± 3.3
J13 (2)	12.7 ± 0.2	5 ± 0.7	0.39 ± 0.05	10 ± 3
N13 (4)	11.3 ± 1.2	4.7 ± 1.3	0.42 ± 0.13	6.3 ± 1.9

Fig. 4. Daily mean precipitations in 2012 (a) and 2013 (b). Light grey inserts represent the three field campaigns.

Table 3
Individual values for pH and $[NH_4^+]$, Γg and χ_g. $[NH_4^+]$ has not been measured in July 2013, but deduced from total N ($[NH_4^+] = 0.06 \times TotN$, as calculated from 2012 values).

Period	Date	pH	$[NH_4^+]$ mg/kg	Γg $[NH_4^+]/[H^+]$	χ_g (ppb)
J12	11/07/2012	6.52–6.79	2.5–12.9	689–6628	16–150
	12/07/2012	6.55–6.76	1.85–4.09	547–1961	14–50
	13/07/2012	6.16–6.48-6.49	1.35–2.21-3.61	347-434-556	9-12-15
	14/07/2012	6.21–6.26-6.47	1.67–1.79-1.88	254-271-410	7-8-12
J13	11/07/2012	5.77–6.3-6.61	2.15-2.55-5.63	276-358-865	8-11-27
N13	31/10/2013	7.43	0.86	1940	56
	01/11/2013	7.07–7.08	0.66–3.16	667–3094	18–86
	05/11/2013	7.28	2.42	3800	106

and management as well as growth stage throughout the season (Riedo et al., 2002). The main influencing factor seems to be the N input to the ecosystem, coming from both N deposition in high polluted areas or N fertilization in agrosystems (Sutton et al., 1994). In Dahra, the values are in the range of values from arable land in temperate ecosystems with no fertilization (Massad et al., 2010), and close to values calculated by Wentworth et al. (2014) in a non fertilized grassland in Canada. Considering that Dahra is in a non polluted environment (contrary to temperate ecosystems mentioned in the above cited studies), the measured range of emission potential values may be explained by the presence of livestock and the N input to the soil through animal excreta.

The ammonia compensation point in the soil ranges between 7 and 150 ppb, with soil temperatures between 32 and 37 °C. Following Nemitz et al. (2001), large compensation point mixing ratios are found for large emission potentials. The soil samples used for pH and ammonium analysis reflect a high spatial heterogeneity, and give a large range of compensation points. However, such high values of compensation point seem overestimated, which may be explained by the fact that the Nemitz et al. (2001) parameterization for compensation point calculation has not been tested in hot semi arid conditions. This assumption would however necessitate more sample analysis to be confirmed.

3.4. NO, N₂O, NH₃ fluxes

3.4.1. NH₃ fluxes

Results in Figs. 5–7 show daily averaged NH₃ fluxes (± 1 standard deviation) in ngN m^{-2} s^{-1}, for J12, J13 (beginning of wet season) and N13 (end of wet season) respectively. The number of individual fluxes used for daily averages is comprised between 6

and 26, depending on the day.

The first strong feature of these figures is illustrated by the extended standard deviation in J12 (Fig. 5) and J13 (Fig. 6). Indeed, the spatial variability of the fluxes was high and fluxes could alternate rapidly between positive and negative values within a short time interval (15–30 min). In N13 (Fig. 7), standard deviations are smaller, showing more stable positive fluxes, giving a net emission from the soil to the atmosphere.

The second strong feature is that the NH₃ fluxes are rather low, with mean campaign averages of 1.3 ± 1.1 ngN m^{-2} s^{-1} in J12, -0.1 ± 1.1 ngN m^{-2} s^{-1} in J13, and 0.7 ± 0.5 ngN m^{-2} s^{-1} in N13. The differences in average SOC content and total nitrogen between the three campaigns are not significant (Table 2 and paragraph III-2), and the differences in ammonia exchanges could not be related to SOC and N contents.

In J12, the large soil emission potential and soil $[NH_4^+]$ (Table 3) at the beginning of the field campaign could explain the positive fluxes on 11 and 12 July. However, despite the decrease in soil $[NH_4^+]$, NH₃ fluxes remain highly positive until 15 July and decrease afterwards. High positive fluxes could be associated with larger soil moisture in J12 (Fig. 3), favoring microbial activity in the soil. Indeed, J12 fluxes at the beginning of the campaign are influenced by rain events which occurred before. The cumulative precipitation calculated 5 days before J12 campaign is 66 mm, whereas it is only 0.15 mm 5 days before the J13 and N13 campaigns. The residual water content at the beginning of J12 campaign is therefore totally different and explains the differences of flux behavior between the campaigns.

NH₃ concentrations have been measured in ambient air. In J12, $[NH_3] = 8.8 \pm 3.3$ ppb is smaller than the mean compensation point (between 7 and 150 ppb, Table 3), and leads to intermediate

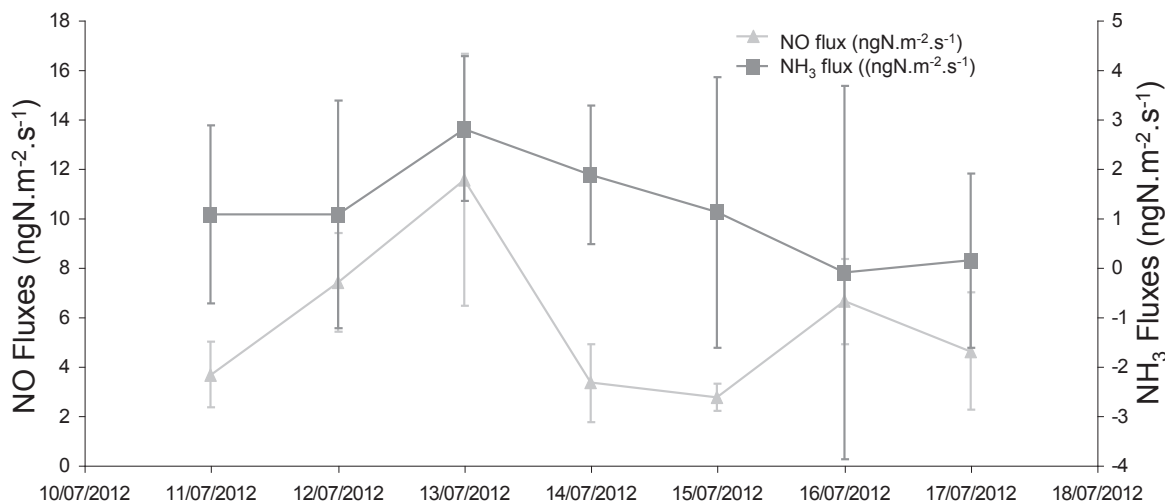**Fig. 5.** Daily NO and NH₃ fluxes in ng m^{-2} s^{-1} in July 2012. Vertical bars show the standard deviation from individual fluxes.

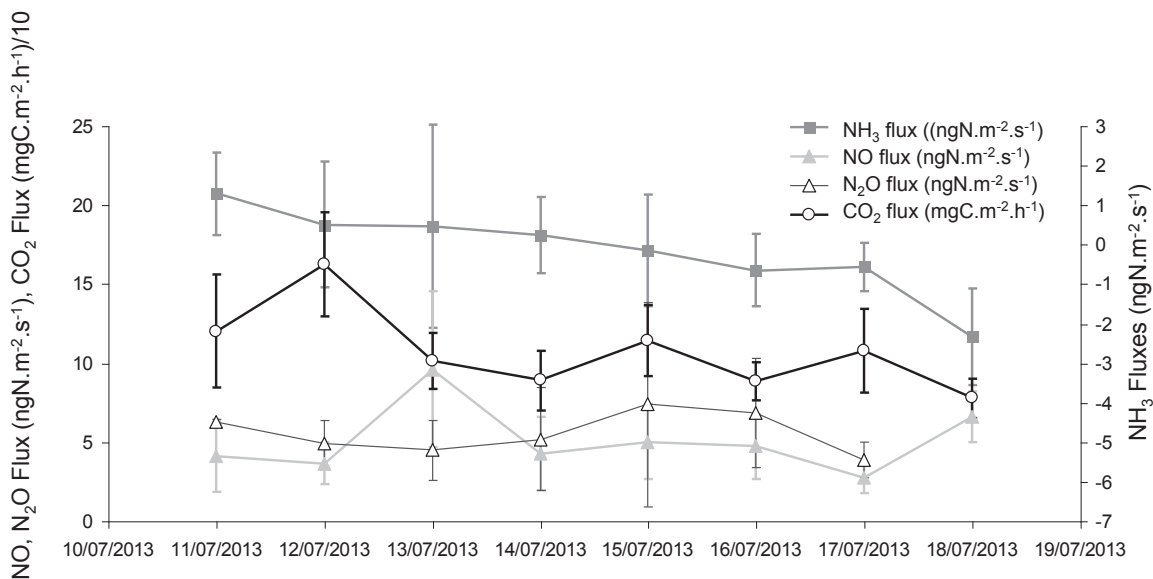**Fig. 6.** Daily NO, N_2O and NH_3 fluxes in ng m^{-2} s^{-1}, CO_2 fluxes mgC m^{-2} h^{-1} in July 2013. Vertical bars show the standard deviation from individual fluxes. CO_2 fluxes are divided by 10.
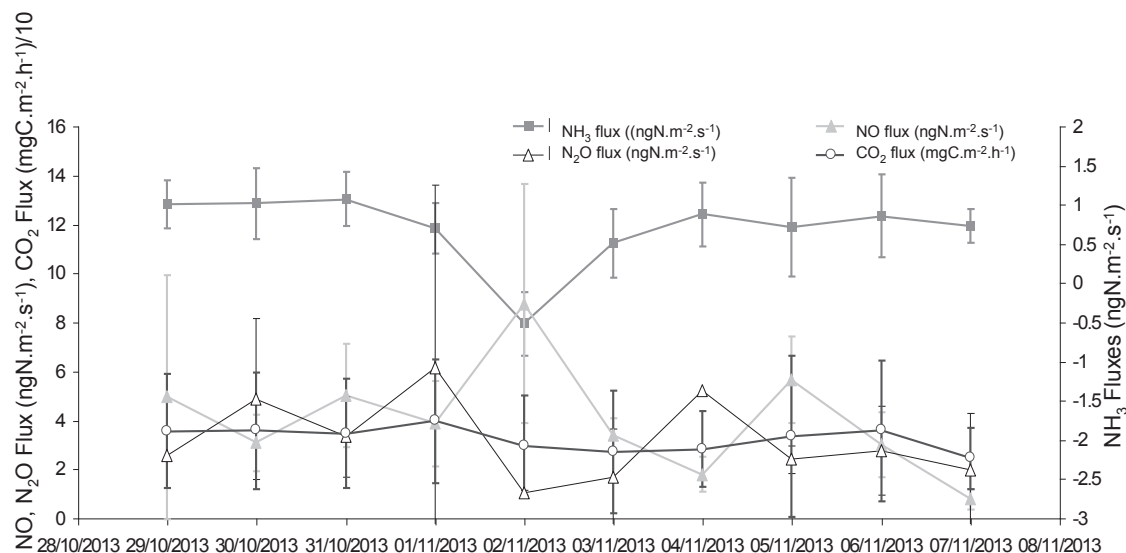

Fig. 7. Daily NO, N_2O and NH_3 fluxes in ng m^{-2} s^{-1}, CO_2 fluxes mgC m^{-2} h^{-1} in November 2013. Vertical bars show the standard deviation from individual fluxes. CO_2 fluxes are divided by 10.

ammonia emission. In J13, $[NH_3] = 10 \pm 3$ ppb and gets in the range of the compensation point value (between 8 and 27), explaining a change from emission to deposition processes. The resulting flux is close to 0, and the daily means show a continuous transition from positive (1.3 ngN m^{-2} s^{-1}) to negative (-2.3 ngN m^{-2} s^{-1}) fluxes between the beginning and the end of the campaign, suggesting a transition period for exchange processes, associated with the setting of the wet season. In N13, $[NH_3] = 6.3 \pm 1.9$ ppb is far less than the compensation point (between 18 and 106 ppb), and ammonia emission dominates, despite low soil moisture.

A multiple linear regression analysis was performed between daily means of NH_3 fluxes for the three periods and all relevant available parameters, as mentioned in the method section (II-7). The best multiple linear regression model is found with soil moisture at 5 cm depth, and air humidity at 2 m height, with a

determination coefficient $R^2 = 0.24$ (p < 0.05). This result enhances the fact that soil moisture and air humidity variations are responsible for changes between NH_3 deposition to NH_3 emission (and *vice versa*) in a 24% proportion, considering that NH_3 exchanges are reduced in low moisture conditions, and that NH_3 is highly soluble in water.

These NH_3 fluxes are in the lower range of fluxes measured in semi arid regions, *e.g.* McCalley and Sparks, (2008) measured NH_3 emission between 0.9 and 10 ngN m^{-2} s^{-1} in the Mojave Desert, and Schaeffer et al. (2003) have measured NH_3 volatilization around 2.0 ± 0.3 ngN m^{-2} s^{-1} in the same area. Fluxes of NH_3 over non fertilized grasslands have been measured in Canada (Wentworth et al., 2014) (fluxes around -5.8 ± 3 and 2.6 ± 4.5 ngN m^{-2} s^{-1}, depending on the season), or inferred (Wichink Kruit et al., 2007, fluxes ranging from -24 to 4 ngN m^{-2} s^{-1}, depending on

meteorological variations), in the Netherlands. Both these sites give higher fluxes than in the present study, but this could be explained by the geographical location of the fields in temperate regions, probably influenced by high nitrogen inputs in the past or high nitrogen loads from dry deposition.

3.4.2. Effect of rainfall on NH_3 fluxes

A 20 mm rainfall event was simulated on 15 July 2013 and 4 November 2013. Flux measurements were performed on 16, 17 and 18 July, 4 and 7 November (Fig. 8a). In July 2013, NH_3 fluxes are characterized by a high variability the day after watering (0.6 ± 5.2 ngN m^{-2} s^{-1} on the 16 July), showing the change between emission and deposition fluxes, and decrease to a mean deposition flux already two days after watering. In November 2013, NH_3 fluxes average 9.0 ± 2.6 ngN m^{-2} s^{-1} the day of watering and decrease to 3.3 ± 0.7 ngN m^{-2} s^{-1} 3 days after, still a relatively high emission value compared to mean November fluxes without watering. The 4 November, NH_3 fluxes increase by a factor of 10 between dry and wet soils, and by a factor of 4 on the 7 November, compared to the daily mean fluxes measured the same day on dry soils.

3.4.3. NH_3 emission from the litter

Ammonium content was measured in N13 in 3 samples of standing straw. [NH_4^+] is 100 ± 72 mg/kg, and mean total N is 10 ± 3 g/kg. Compared to soil N and soil ammonium content, these values are 30 times higher, and are probably the cause of NH_3 release to the atmosphere, even with low residual humidity. Apart from fertilizer-induced NH_3 volatilization, significant emissions may also occur from soil in barren land and in senescent plant canopies where litter on the soil surface, and senescent leaves contribute to emissions (Sutton et al., 2007, 2009, 1994; Massad et al., 2010; David et al., 2009). For the litter, it has been assumed that the amount of [NH_4^+] released to the atmosphere as NH_3 is controlled by the litter [NH_4^+], by litter water content, and by mineralization and nitrification rates (Nemitz et al., 2000). NH_3 emission from leaves is due to biochemical processes inside the leaf (stomatal release), and to microbial decomposition processes at the leaf surface by microorganisms (Farquhar et al., 1979). These processes involved in litter emission are confirmed by high ammonium and total N content measured in a few samples of standing straw in Dahra. While litter may be mainly considered as a source of NH_3 (contrary to plant and soil which may be a source or a sink, Massad et al., 2008), dry litter is a much smaller source than wet litter (David et al., 2009). In N13, soil moisture is low, and soil and litter remain small emitters of NH_3. The availability of NH_4^+ content in litter leads to stronger emission after watering due to enhanced decomposition of litter. The availability of nutrients is slowed down by the effective low water content in N13. However, considering that soil NH_4^+ content is lower in N13 (1.6 ± 1.1 mg/kg, compared to 3.4 ± 3.4 and 2.3 ± 0.3 in J12 and J13 respectively), it is possible to conclude that litter remains the main source of NH_3 emission in N13, even with low water content. These emissions contribute significantly to soil emissions and need to be taken specifically into account (Nemitz et al., 2001; Denmead et al., 1976).

3.4.4. NO fluxes

Figs. 5—7 show NO fluxes from soils in ngN.m^{-2}. s^{-1}, in J12, J13 and N13 respectively. Averages are 5.7 ± 3.1 ngN m^{-2} s^{-1} in J12,

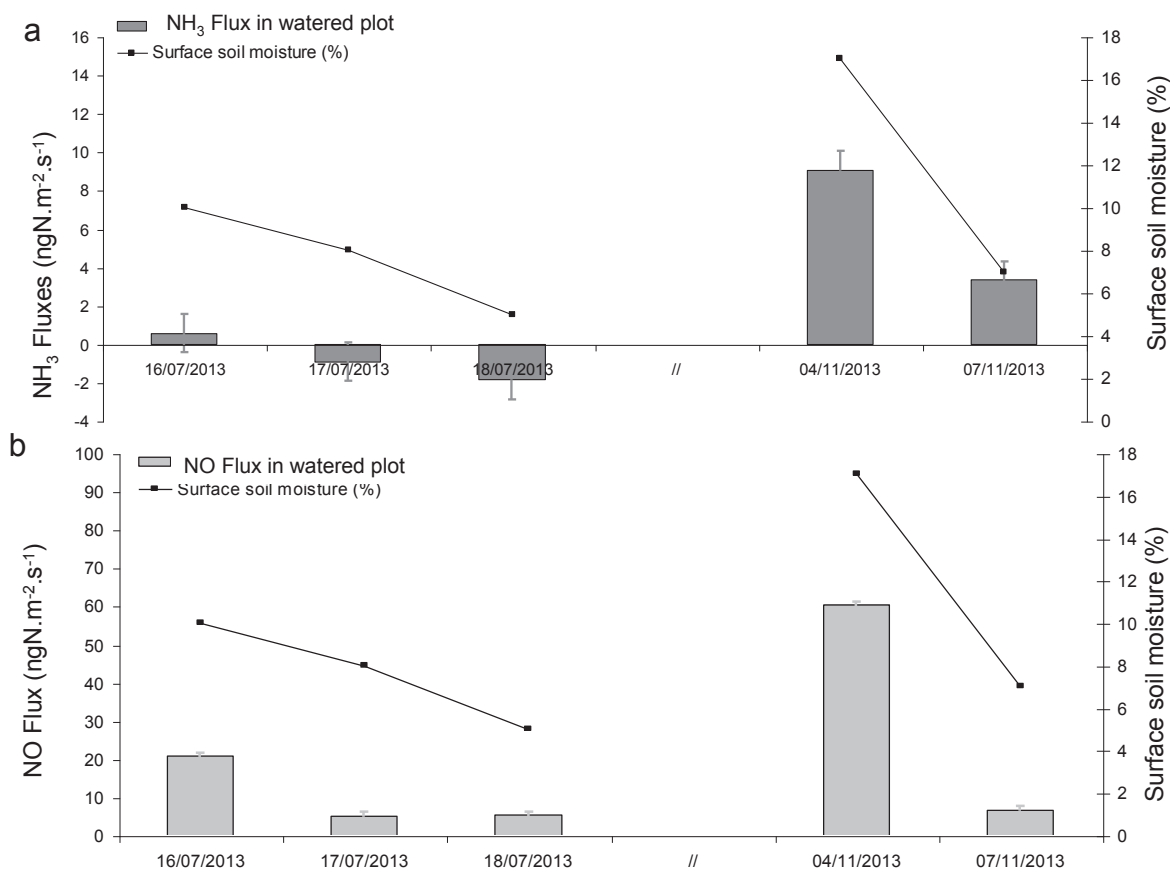**Fig. 8.** Daily NO (a) and NH_3 fluxes (b) in ng m^{-2} s^{-1} in July and November 2013, from artificially watered plots, with soil surface moisture. Vertical bars show the standard deviation from individual fluxes.

5.1 ± 2.1 ngN m^{-2} s^{-1} in J13, and 4.0 ± 2.2 ngN m^{-2} s^{-1} in N13. Statistically, the flux differences between the three periods are not significant (p > 0.05). However, the mean NO flux value in J12 is larger than during the other periods, and could be partly explained by larger mean soil moisture in J12. Indeed, mean soil moistures are significantly different between periods. As a comparison, NO fluxes have been measured in South African grassland by Serça et al. (1998) and averaged around 3.4 ngN m^{-2} s^{-1}during the dry season, and Meixner et al. (1997) measured fluxes around 4.4 ngN m^{-2} s^{-1} during the wet season, and 1.2 ngN.m^{-2}. s^{-1} during the dry season (volumetric soil moisture values below 1.5%). NO fluxes have also been measured in a comparable dry savanna in Agoufou (Mali), with equivalent soil texture and vegetation cover as in Dahra, and fluxes reached 6.7 ± 2.4 ngN m^{-2} s^{-1} in July 2004 (beginning of wet season), and 2.3 ± 0.8 ngN m^{-2} s^{-1} in August 2005 (Delon et al., 2015).

As for NH$_3$ fluxes, NO emission increases during the first three days of the 2012 campaign, following a rainfall event on 9 July. Afterwards, fluxes decrease and remain low, which is consistent with the well known pulse effect of NO, induced by an excess of mineralization when the dry soil is suddenly wetted by a rainfall event. Indeed, mineral and organic substrates tend to accumulate at the soil surface and in the soil during the long dry season (Austin et al., 2004), and release large quantities of NO when the soil moisture reaches a sufficient threshold (Schwinning et al., 2004; Pilegaard, 2013). This pulse effect may be explained by a balance between the nutrient availability to the microorganisms and the diffusion of oxygen (Brümmer et al., 2008). In J13, the soil humidity was low and no clear tendency over time can be seen (Fig. 6). A larger flux with a larger standard deviation is seen on 13 July, enhancing the high spatial variability and the possible presence of acacia roots in the chamber, boosting the soil N availability and the N release (Ludwig et al., 2001; Erickson et al., 2002).

Stepwise multiple regression analysis between daily NO fluxes and daily relevant parameters was performed. The best model is found for NO flux with air humidity at 2 m height and soil moisture at 5 cm depth, with R^2 being 0.2 (p = 0.08). This score is improved if the three parameters are used as log values, with R^2 = 0.38 (p < 0.01). This score remains low, probably because of non significant differences of NO fluxes between periods. However, soil moisture and air humidity are highlighted by the statistical results as main relevant parameters to explain NO fluxes, as expected for soil moisture. Air humidity and soil moisture are closely linked (R^2 = 0.8, p < 0.001), as shown in Fig. 3a and b, and the regression analysis reveals a coupled influence of both humidity on NO fluxes.

The differences of total N are not significant between the three periods (see paragraph III-2). However, N contents are larger than in other comparable savanna ecosystems: 0.15 g//kg in the Fakara region, Niger (Turner and Hiernaux, 2015), 0.11 g/kg in the Gourma region, Mali, (Diallo and Gjessing, 1999), 0.12 g/kg in Agoufou, Mali (Mougin, unpublished data). As discussed in Erickson et al. (2002), the N availability is a major factor in influencing NO and N$_2$O (and NH$_3$) emissions. Equivalent N content in soil during the three campaigns may partly explain the close values of fluxes between periods, even if soil moisture in N13 is lower. In N13, fluxes are less scattered than in J12 and J13, showing lower spatial variation during that campaign as for NH$_3$ emissions. The spatial heterogeneity may be explained by the presence of livestock and the short term history of the Dahra site, *i.e.* how livestock has trampled, grazed and excreted during the different seasons, which may influence the SOC and N stock quality.

Mean soil temperatures were significantly different between J12 (33.9 °C) and J13 (36.8 °C), and between J13 and N13 (34.4 °C, p < 0.05), but were not significantly different between J12 and N13. Soil temperature was not highlighted as an influencing parameter

by regression analysis for NO fluxes. This could be due to the fact that soil temperatures for the three periods are above the optimum temperatures involved in nitrification processes causing NO emission. As a matter of fact, changes in temperature will not affect nitrification rates (Bai et al., 2013) and low soil moisture levels hide the potential temperature effect.

The presence of vegetation should also have an influence on NO emissions, as demonstrated by Feig et al. (2008) and references therein, particularly through N uptake by plants. The difference between sparse and short (1 or 2 cm) green growing vegetation in J12 and J13, and high standing straw in N13 should lead to a change in physical characteristics of the surface, influencing the fluxes. But in J12 and J13 N uptake by plants in this period of intense growth is still limited due to the very low vegetation cover. Moreover, the rainy season is not well established, and periods between rain events are still long (>5 days, see Fig. 4). In N13, the N in the soil is no more required for vegetation growth, and is available for release to the atmosphere. Therefore, N uptake by plants and N release to the atmosphere are not in competition for soil N content in the results presented here. Main influencing parameters will be soil moisture and N content.

3.4.5. Link between NO emission and soil respiration (CO$_2$ fluxes)

CO$_2$ fluxes were measured in J13 and N13 (Figs. 6 and 7 respectively). Averages are 107 ± 26 mg C.m^{-2}. h^{-1} in J13, and 32 ± 5 mg C.m^{-2}. h^{-1} in N13. These estimates are close to eddy covariance based ecosystem respiration measurements made at the Dahra site by Tagesson et al. (2015a). They estimated ecosystem respiration to be 103 ± 29 mgC.m^{-2}. h^{-1} in J13 and 21.4 ± 18 mgC.m^{-2}. h^{-1} in N13 for the same periods as the field campaigns. The higher flux values during J13 could be explained by the rapid response of the soil decomposers to the increase in soil moisture at the beginning of the rainy season (June–July), by the intense decomposition of the litter buried during the dry season (Tagesson et al., 2015a) and possibly by the autotrophic respiration of the growing vegetation. However, heterotrophic respiration remains the main origin of the CO$_2$ release in J13. At that time of the year, ecosystem respiration dominates the net ecosystem CO$_2$ exchange and the ecosystem is a strong C source (Tagesson et al., 2015a). July CO$_2$ fluxes are comparable to daily values measured in a semi arid fallow and a millet field in Niger before the start of the vegetation growth at the beginning of the wet season (100–200 mg C.m^{-2}. h^{-1}, Boulain et al., 2009). Dahra fluxes may be explained by large C and N contents for semi natural lands (Table 2). They compare well with fluxes measured in cultivated areas reaching 250 mgC.m^{-2}. h^{-1} at the core of the wet season in a Sudanian climate (Ago et al., 2014). As a comparison with another type of ecosystem, some larger respiration fluxes (200–600 mg C.m^{-2}. h^{-1}) were measured in tropical C4 wetland plants close to Lake Victoria (Uganda) due to the decomposition of organic matter at the wetland surface (Saunders et al., 2012).

In N13, despite the presence of dry standing straw, CO$_2$ respiration is low. The vegetation is brown and there is no more autotrophic activity in the herbaceous layer, while a low maintenance respiration by the roots may be maintained if root residues persist. Additionally, soil moisture content is low which tends to lower the heterotrophic activity. Traoré et al. (2015) measured equivalent daily fluxes in the northern Burkina Faso, between 25 and 35 mgC.m^{-2}. s^{-1}, at the beginning of the dry season, and Ago et al. (2014) measured 80 mgC.m^{-2}. s^{-1} in Benin at the same period in a cultivated savanna. These authors have found that respiration is highly dependent on soil moisture. In our study, it also appears to be the determinant factor at the beginning of the 2013 dry season. Indeed, even if more biomass is present, low soil moisture does not allow litter decomposition and subsequent heterotrophic

respiration. Soil temperature and biomass quantity are not emphasized as driving factors at this period.

When shifting the NO fluxes by one day, the correlation coefficient between NO fluxes and CO_2 fluxes is $R^2 = 0.6$ in J13, with p-value = 0.03. CO_2 is one day in advance, highlighting the fact that in our measurements the ecosystem respiration precedes the microbial N transformation in the soil, leading to NO release after CO_2 emission. Indeed, the first rains produce a physical effect of diffusion (Moyano et al., 2013), which releases the CO_2 trapped in the soil pores. Afterwards, the rains activate enzymes in the soil which generate the decomposition of organic matter and release CO_2, and microorganisms stimulate the production of NO by nitrification processes. This 1 day lag value should mostly been understood as a close connection between respiration and nitrification processes (Xu et al., 2008), and may be less than one day in other sets of data. For low ecosystem respiration in N13, this process could not be highlighted. N content and soil water content play an essential role in respiration processes, as highlighted through these results and the references cited. Soil respiration and nitrification processes (causing NO release) are closely linked by microbial processes: soil microorganisms trigger soil respiration and decomposition of soil organic matter (Xu et al., 2008).

3.4.6. Effect of rainfall on NO fluxes

A 20 mm rainfall event was simulated on 15 July 2013 and 4 November 2013 to check the NO flux dependence to soil moisture in dry land ecosystems as described in the literature (Austin et al., 2004; Meixner et al., 1997; Yan et al., 2005; Hudman et al., 2010; Jaeglé et al., 2004; Kim et al., 2012; Stewart et al., 2008). As for NH_3, NO flux measurements were performed on 16, 17 and 18 July, 4 and 7 November (Fig. 8b), together with surface soil moisture. The increase of soil moisture has an obvious and rapid effect In July, fluxes are multiplied by 3 the day after watering (20.8 ± 7.8 ngN $m^{-2} s^{-1}$), and decrease to their mean "dry" values already two days after watering. These tendencies are consistent with measurements in South African soils (Levine et al., 1996), giving mean background NO emissions from the dry sites between 0.4 and 6.2 ngN $m^{-2} s^{-1}$ and 4.7 to 34.0 ngN $m^{-2} s^{-1}$ from the wetted sites.

In November 2013, NO fluxes averaged 60.3 ± 26.1 ngN $m^{-2} s^{-1}$ the day of watering (4–7 h after), and decreased to much lower values 3 days after (6.8 ± 3.4 ngN $m^{-2} s^{-1}$). Two essential reasons may explain the more important increase in November than in July: i) measurements were made only a few hours after watering, allowing soil water content to be optimum for NO release, whereas in July, measurements were conducted one day after watering; ii) The presence of standing straw, above soil and buried litter strongly increases the single effect of moisture, and multiplies by 33 the mean dry flux (1.8 ± 0.7 ngN $m^{-2} s^{-1}$ on November 4). First of all, microbial activity, enhanced by increasing soil moisture, is the first important factor on litter decomposition according to measurements and to decomposition models Moorhead and Reynolds, 1991; Parton et al., 2007). Secondly, recent studies indicate that photodegradation caused by UV-B radiation plays a key role in litter and straw decomposition, and on soil C and N cycling in semi arid ecosystems (Liu et al., 2014), increasing N avalability. The role of thermal degradation on C cycle in arid ecosystems has also been highlighted by Van Asperen et al. (2015), and it may be assumed that the N cycle is also impacted by this effect. The cumulative effect of biodegradation and photo/thermal degradation in those particular conditions may explain the strong increase in NO emissions after wetting.

3.4.7. N_2O fluxes

The discussion will only rely on J13 and N13 measurements (Figs. 6 and 7 respectively) as N_2O fluxes were not measured in J12.

Averages are 5.5 ± 1.3 ngN $m^{-2} s^{-1}$ in J13, and 3.2 ± 1.7 ngN $m^{-2} s^{-1}$ in N13. Different reviews on N_2O emissions in semi arid lands show rather low emissions, between 0.2 and 1.0 ngN $m^{-2} s^{-1}$ in South Africa and Colorado during dry the season, and between 1.0 and 2.9 ngN $m^{-2} s^{-1}$ during the wet season (Meixner and Yang, 2006). Castaldi et al. (2006) report null or very low emissions (<0.3 ngN $m^{-2} s^{-1}$) in semi arid savannas. Brümmer et al. (2008) show measured N_2O fluxes around 1.4 ngN $m^{-2} s^{-1}$ in Burkina Faso, with WFPS below 7%. At the onset of the rain season, fluxes reach 5 ngN.m^{-2}. s^{-1} with WFPS = 20%, comparable to WFPS that could be found in Dahra in July.

Stepwise multiple regression analysis allowed to find a model between N_2O fluxes and soil moisture at 5 cm depth, with $R^2 = 0.15$ (p < 0.01). Larger fluxes in J13 than in N13 are consistent with slightly larger soil moisture, but this parameter only explains 15% of the variance. N_2O fluxes are supposed to depend also on soil mineral nitrogen content, but this parameter could not be related to N_2O fluxes in this statistical study, due to differences in the time steps of samples collection. Soil temperature did not appear as a driving parameter for N_2O fluxes, because even with significant differences between seasons, temperatures are above the optimum needed to influence denitrification and nitrification processes (Bai et al., 2013).

N_2O flux values are close to NO flux values, whereas generally denitrification processes in the soil causing N_2O release are supposed to be small compared to nitrification processes in dry sandy soils causing NO emissions. In theory, N_2O emission increases with the soil water content because the oxygen availability in soils is regulated by soil moisture, and drives the way microbes recycle N in the soils (Oswald et al., 2013). Anderson and Levine (1986) suggest that N_2O emission from soil takes place in a more restricted range of soil moisture conditions than does NO emission, and therefore should occur less frequently in dry soils. The regulation of enzyme synthesis behind N_2O production and consumption in the soil is principally driven by O_2 partial pressure (i.e. water filled pore space, WFPS) and concentrations of nitrogen substrates (Conrad, 1996). There are also bacteria that denitrify under aerobic conditions, highlighting the existence of aerobic denitrification (Robertson and Kuenen, 1984) and showing that the alternation between aerobic/anaerobic conditions occurs frequently at small scale (Lloyd et al., 1987). This process of aerobic denitrification may occur in Dahra. Another possible explanation for important N_2O fluxes found in Dahra could be that, according to Meixner and Yang (2006), it is still difficult to assess the importance of nitrification versus denitrification for the exchange of NO and N_2O. They mention that the main contribution to N_2O fluxes arises from below 0.5 m depth, whereas production and consumption zones for NO are located closer to the surface (above 0.1 m). However other authors have provided experimental evidence that N_2O could also be produced above 0.03 m (Neftel et al., 2000). It is therefore difficult to establish the optimal depth for denitrification.

An alternative metabolic process for producing N_2O in low moisture soils is the nitrifier denitrification of ammonia by oxidizing bacteria (Butterbach-Bahl et al., 2013). This biochemical pathway could be a major contributor in N_2O production; thus, N_2O could also be produced in low soil moisture conditions. As a consequence, the possible influence of soil moisture below the surface (where N_2O is produced) during the wet season, the potential aerobic denitrification in microsites, and the nitrifier denitrification, added to nitrification processes, may explain the high N_2O emissions in Dahra.

The NO/N_2O ratio is a way to discriminate between nitrification and denitrification processes in the soil, causing the N release. It is generally assumed that a ratio well below 1 means that denitrification is the main pathway of N-trace gas production (Anderson

and Levine, 1986). Other studies found that nitrification occurs when NO/N$_2$O is superior to 0.11 (Meijide et al., 2007; Zhang et al., 2011). In J13, 86% (6/7 daily averages) of the NO/N$_2$O ratio are below 1, 14% above 1 (1/7 daily average). In N13, 40% (4/10 daily averages) of the NO/N$_2$O ratio are below 1, 60% above 1 (6/10 daily averages). All ratios in the present study are above 0.34, leading to the conclusion that nitrification may be an important process involved in both NO and N$_2$O production and release, and complementary to the assumption that denitrification may still occur in depth and at surface through aerobic pathways. It has been suggested in Smith & Tiedje (1979) that synthesis of nitrate and nitrite reductase (causing NO release) starts within hours whereas synthesis of nitrous oxide reductase may be delayed for more than 1 day, so that N$_2$O is produced after NO. Both processes are therefore involved in NO and N$_2$O release in Dahra.

The relationship between NO and NH$_3$ fluxes is linked to the biological activity in the soil. It appears that at Dahra, in the absence of rain, volatilization of NH$_3$ from soils is low, leading to low emission or even to deposition of NH$_3$. The NH$_4^+$ content in the soil is therefore available for nitrification and for several ways of denitrification processes in the soil which pilot NO and N$_2$O emissions. Some experiments in the Mojave Desert have shown that when conditions are favorable to nitrification, ammonia volatilization is reduced, possibly due to the decrease of ammonium by nitrifiers involving a competition effect between NO and N$_2$O emission, and NH$_3$ volatilization (McCalley and Sparks, 2008).

The simultaneous decrease of NO and N$_2$O emissions in N13 with low soil moisture levels is a positive argument which supports the idea that NO and N$_2$O emission processes are linked and related to soil moisture.

4. Conclusion

NO, NH$_3$, NO$_2$ and CO$_2$ fluxes were investigated through in situ measurements made in a semi arid site in northern Senegal during 3 field campaigns in July 2012, July 2013 and November 2013. Complementary to these exchanges fluxes, soil N and C content, as well as soil moisture, soil temperature and pH, and meteorological data, were measured and used for a better understanding of the intensity of surface fluxes.

The field campaigns were performed during periods of low rainfall, leading to small quantities of N emitted, but still showing that emissions of N compounds are not negligible even at low soil moisture levels. Strong pulses of NH$_3$ and NO have been measured after manually watering the soil, highlighting the immediate release of nitrogen compounds in recently wetted soils with litter and straw. The process of NH$_3$ bi-directional exchange is highlighted throughout the campaigns, showing mean emission in J12 and N13 due to higher compensation point concentrations than mean ambient concentrations. In J13, emission and deposition both occur because compensation point approaches the mean ambient NH$_3$ concentration. The important role of litter and standing straw in emitting ammonia and NO at the end of the rain season has been highlighted, while decomposition of the organic matter is limited due to low soil moisture and low microbial activity. N$_2$O fluxes are equivalent to NO fluxes, suggesting that denitrification occurs even at low soil moisture levels, through aerobic denitrification or nitrifiers denitrification processes, and associated with nitrification processes. CO$_2$ fluxes are 3 times higher in J13 than in N13, probably due to more effective ecosystem respiration at the beginning of the rain season, when microbe populations grow quickly and are active decomposers. The turnover, transformation and flux of reactive nitrogen species is inevitably associated to the activity of soil microorganisms (Ambus et al., 2011), to vegetation growth (root and biomass) and therefore to soil respiration.

This study gives an overview of several processes occurring in semi arid soils, leading to N and C exchange with the atmosphere. N compounds exchange flux processes are often well described in the literature, yet in situ experiments in such regions are lacking preventing detailed knowledge to be gained on the subject. More measurements are nevertheless needed to better understand the underlying mechanisms in the soils affected by drying and rewetting cycles, and affecting N exchanges fluxes with the atmosphere. The contrasted ecosystem conditions due to drastic changes in water availability in semi arid regions have important non linear impacts on the biogeochemical nitrogen cycle and ecosystem respiration (Wang et al., 2015). The soil nitrogen response to water availability in those particular systems needs to be focused on to quantify the nitrogen release to the atmosphere. Our study contributes to an improved regional understanding of this particular climatic system, by giving an insight in remote parts of the Sahel at two contrasted periods of the year. These mechanisms are essential, and may affect the atmospheric chemistry if changes in precipitation regimes occur due to climate change.

References

Adon, M., Galy-Lacaux, C., Yoboué, V., Delon, C., Lacaux, J.P., Castera, P., Gardrat, E., Pienaar, J., Al Ourabi, H., Laouali, D., Diop, B., Sigha-Nkamdjou, L., Akpo, A., Tathy, J.P., Lavenu, F., Mougin, E., 2010. Long term measurements of sulfur dioxe, nitrogen dioxide, ammonia, nitric acid and ozone in Africa using passive samplers. Atmos. Chem. Phys. 10, 7467−7487. http://dx.doi.org/10.5194/acp-10-7467-2010.

Ago, E.E., Agbossou, E.K., Galle, S., Cohard, J.-M., Heinesch, B., Aubinet, M., 2014. Long term observations of carbon dioxide exchange over cultivated savanna under a Sudanian climate in Benin (West Africa). Agric. For. Meteorol. 197, 13−25.

Akiyama, H., McTaggart, I.P., Ball, B.C., Scott, A., 2004. N$_2$O, NO, AND NH$_3$ emissions from soils after the application of organic fertilizers, urea and water. water. Air, Soil Pollut. 156, 113−129.

Almand-Hunter, B.B., Walker, J.T., Masson, N.P., Hafford, L., Hannigan, M.P., 2015. Development and validation of inexpensive, automated, dynamic flux chambers. Atmos. Meas. Tech. 8, 267−280.

Ambus, P., Skiba, U., Butterbach-Bahl, K., Sutton, M.A., 2011. Reactive nitrogen and greenhouse gas flux interactions in terrestrial ecosystems. Plant Soil 343, 1−3.

Anderson, I.C., Levine, J.S., 1986. Relative rates of nitric oxide and nitrous oxide production by nitrifiers, denitrifiers, and nitrate respirers. Appl. Environ. Microbiol. 938−945.

Arneth, A., Mercado, L., Kattge, J., Booth, B.B.B., 2012. Future challenges of representing land-processes in studies on land-atmosphere interactions. Biogeosciences 9, 3587−3599.

Austin, A.T., Yahdjian, L., Stark, J.M., Belnap, J., Porporato, A., Norton, U., Ravetta, D.A., Schaeffer, S.M., 2004. Water pulses and biogeochemical cycles in arid and semi arid ecosystems. Oecologia 141, 221−235.

Assouma, M.H., Vayssières, J., Serça, D., Guerin, F., Blanfort, V., Lecomte, P., Traoré, I., Ickowicz, A., Manlay, R.J., Bernoux, M., 2016. Livestock induces strong spatial heterogeneity of soil CO$_2$, N$_2$O, CH$_4$ emissions within a semi-arid sylvo-pastoral landscape in West Africa. J. Arid Land. http://dx.doi.org/10.1007/s40333-016-0099-3.

Bai, E., Li, S., Xu, W., Li, W., Dai, W., Jiang, P., 2013. A meta-analysis of experimental warming effects on terrestrial nitrogen pools and dynamics. New Phytol. 199, 441−451. http://dx.doi.org/10.1111/nph.12252.

Boulain, N., Cappelaere, B., Ramier, D., Issoufou, H.B.A., Halilou, O., Seghieri, J., Guillemin, F., Oï, M., Gignoux, J., Timouk, F., 2009. Towards an understanding of coupled physical and biological processes in the cultivated Sahel − 2. Vegetation and carbon dynamics. J. Hydrol. 375, 190−203.

Bouwman, A.F., Boumans, L.J.M., Batjes, N.H., 2002. Emissions of N$_2$O and NO from fertilized fields: summary of available measurement data. Glob. Biogeochem. Cycles 16 (4), 1058. http://dx.doi.org/10.1029/2001GB001811.

Brümmer, C., Brüggemann, N., Butterbach-Bahl, K., Falk, U., Szarzynski, J., Vielhauer, K., Wassmann, R., Papen, H., 2008. Soil-atmosphere exchange of N2O

and NO in near-natural savanna and agricultural land in Burkina Faso (W. Africa). Ecosystems 11, 582—600.

Butterbach-Bahl, K., Kock, M., Willibald, G., Hewett, B., Buhagiar, S., Papen, H., Kiese, R., 2004. Temporal variations of fluxes ofNO, NO₂, N₂O, CO₂, and CH₄ in a tropical rain forest ecosystem. Glob. Biogeochem. Cycles 18. http://dx.doi.org/10.1029/2004GB002243. GB3012.

Butterbach-Bahl, K., Baggs, E.M., Dannenmann, M., Kiese, R., Zechmeister-Boltensternb, S., 2013. Nitrous oxide emissions from soils: how well do we understand the processes and their controls? Phil Trans. R. Soc. B 368, 20130122.

Castaldi, S., Ermice, A., Strumia, S., 2006. Fluxes of N₂O and CH₄ from soils of savannas and seasonally-dry ecosystems. J. Biogeogr. 33 (Issue 3), 401—415.

Chapin, F.S., Matson, P.A., Mooney, H.A., 2002. Principles of Terrestrial Ecosystem Ecology. Springer, New York, NY.

Conrad, R., 1996. Soil microorganisms as controllers of atmospheric trace gases (H₂, CO, CH₄, OCS, N₂O, and NO). Microbiol. Rev. 60, 609—640.

Dari-Salisburgo, C., Di Carlo, P., Giammaria, F., Kajii, Y., D'Altorio, A., 2009. Laser induced fluorescence instrument for NO₂ measurements: observations at a central Italy background site. Atmos. Environ. 43, 970—977.

David, M., Loubet, B., Cellier, P., Mattsson, M., Schjoerring, J.K., Nemitz, E., Roche, R., Riedo, M., Sutton, M.A., 2009. Ammonia sources and sinks in an intensively managed grassland canopy. Biogeosciences 6, 1903—1915.

Davidson, E.A., 1991. Fluxes of nitrous oxide and nitric oxide from terrestrial ecosystems. In: Rogers, J.E., Whitman, W.B. (Eds.), Microbial Production and Consumption of Greenhouse Gases: Methane, Nitrogen Oxides and Halomethanes. American Society for Microbiology, Washington, pp. 219—235.

Delon, C., Serça, D., Boissard, C., Dupont, R., Dutot, A., Laville, de Rosnay, P., Delmas, R., 2007. Soil NO emissions modelling using artificial neural network. Tellus 59B, 502—513.

Delon, C., Reeves, C.E., Stewart, D.J., Serça, D., Dupont, R., Mari, C., Chaboureau, J.-P., Tulet, P., 2008. Biogenic nitrogen oxide emissions from soils — impact on NOx and ozone over West Africa during AMMA (African Monsoon Multidisciplinary Experiment): modelling study. Atmos. Chem. Phys. 8, 2351—2363. http://dx.doi.org/10.5194/acp-8-2351-2008.

Delon, C., Mougin, E., Serça, D., Grippa, M., Hiernaux, P., Diawara, M., Galy-Lacaux1, C., Kergoat, L., 2015. Modelling the effect of soil moisture and organic matter degradation on biogenic NO emissions from soils in Sahel rangeland (Mali). Biogeosciences 12, 3253—3272.

Denmead, O.T., Freney, J.R., Simpson, 1976. J. R.: a closed ammonia cycle within a plant canopy. Soil Biol. biochem. 8, 161—164.

Diallo, Gjessing, 1999. Natural Resources Management: Morphopedology in Gourma Region. SSE Research Program Mali-Norway (In French). CNRST-IER-Oslo University, Norway, pp. 1—19.

Dunlea, E.J., Herndon, S.C., Nelson, D.D., Volkamer, R.M., San Martini, F., Sheehy, P.M., Zahniser, M.S., Shorter, J.H., Wormhoudt, J.C., Lamb, B.K., Allwine, E.J., Gaffney, J.S., Marley, N.A., Grutter, M., Marquez, C., Blanco, S., Cardenas, B., Retama, A., Ramos Villegas, C.R., Kolb, C.E., Molina, L.T., Molina, M.J., 2007. Evaluation of nitrogen dioxide chemiluminescence monitors in a polluted urban environment. Atmos. Chem. Phys. 7, 2691—2704.

Elberling, B., Fensholt, R., Larsen, L., Petersen, A.I.S., Sandholt, I., 2003. Water content and land use history controlling soil CO2 respiration and carbon stock in savanna soil and groundnut fields in semi-arid Senegal. Geografisk Tidsskrift-Danish J. Geogr. 103 (2), 47—56. http://dx.doi.org/10.1080/00167223.2003.10649491.

Erickson, H., Davidson, E.A., Keller, M., 2002. Former land-use and tree species affect nitrogen oxide emissions from a dry tropical forest. Oecologia 130, 297—308.

FAO (Food and Agriculture Organization), LCCS (Land Cover Classification System), 2000. Produced by: Natural Resources Management and Environment Department. http://www.fao.org/docrep/003/x0596e/x0596e01f.htm.

Farquhar, G.D., Wetselaar, R., Firth, P.M., 1979. Ammonia volatilization from senescing leaves of maize. Science 203, 1257—1258.

Farquhar, G.D., Firth, P.M., Wetselaar, R., Weir, B., 1980. On the gaseous exchange of ammonia between leaves and the environment: determination of the ammonia compensation point. Plant Physiol. 66, 710—714.

Feig, G.T., Mamtimin, B., Meixner, F.X., 2008. Soil biogenic emissions of nitric oxide from a semi-arid savanna in South Africa. Biogeosciences 5, 1723—1738. http://dx.doi.org/10.5194/bg-5-1723-2008.

Fensholt, R., Sandholt, I., 2005. Evaluation of MODIS and NOAA AVHRR vegetation indexes with in situ measurements in a semi-arid environment. Int. J. Remote Sens. 26, 2561—2594.

Fensholt, R., Sandholt, I., Stisen, S., 2006. Evaluating MODIS, MERIS, and VEGETATION—vegetation indexes using in situ measurements in a semiarid environment. IEEE Trans. Geosci. Remote Sens. 44 (7), 1774—1786.

Flechard, C.R., Fowler, D., 1998a. Atmospheric ammonia at a moorland site. I: the meteorological control of ambient ammonia concentrations and the influence of local sources, Q. J. Roy. Meteor. Soc. 124, 733—757.

Flechard, C.R., Fowler, D., 1998b. Atmospheric ammonia at a moorland site. II: long-term surface-atmosphere micrometeorological flux measurements, Q. J. Roy. Meteor. Soc. 124, 759—791.

Flechard, C.R., Fowler, D., Sutton, M.A., Cape, J.N., 1999. A dynamic chemical model of bi-directional ammonia exchange between semi-natural vegetation and the atmosphere, Q. J. Roy. Meteor. Soc. 125, 2611—2641.

Flechard, C.R., Massad, R.-S., Loubet, B., Personne, E., Simpson, D., Bash, J.O., Cooter, E.J., Nemitz, E., Sutton, M.A., 2013. Advances in understanding, models and parameterizations of biosphere-atmosphere ammonia exchange.

Biogeosciences 10, 5183—5225.

Frank, D.A., Evans, R.D., 1997. Effects of native grazers on grassland N cycling in yellowstone national park. Ecology 78 (7), 2238—2248.

Fuzzi, S., Baltensperger, U., Carslaw, K., Decesari, S., Denier van der Gon, H., Facchini, M.C., Fowler, D., Koren, I., Langford, B., Lohmann, U., Nemitz, E., Pandis, S., Riipinen, I., Rudich, Y., Schaap, M., Slowik, J.G., Spracklen, D.V., Vignati, E., Wild, M., Williams, M., Gilardoni, S., 2015. Particulate matter, air quality and climate: lessons learned and future needs. Atmos. Chem. Phys. 15, 8217—8299. http://dx.doi.org/10.5194/acp-15-8217-2015.

Galy-Lacaux, C., Modi, A.I., 1998. Precipitation chemistry in the sahelian savanna of Niger, Africa. J. Atmos. Chem. 30, 319e343.

Grote, R., Lehmann, E., Brümmer, C., Brüggemann, N., Szarzynski, J., Kunstmann, H., 2009. Modelling and observation of biosphere—atmosphere interactions in natural savannah in Burkina Faso, West Africa. Phys. Chem. Earth 34, 251—260.

Gut, A., van Dijk, S.M., Scheibe, M., Rummel, U., Welling, M., Ammann, C., Meixner, F.X., Kirkman, G.A., Andreae, M.O., Lehmann, B.E., 2002. NO emission from an Amazonian rain forest soil: continuous measurements of NO flux and soil concentration. J. Geophys. Res 107 (D20), 8057. http://dx.doi.org/10.1029/2001JD000521.

Hertel, O., Reis, S., Skjoth, C.A., Bleeker, A., Harrison, R., Cape, J.N., Fowler, D., Skiba, U., Simpson, D., Jickells, T., Baker, A., Kulmala, M., Gyldenkaerne, S., Sorensen, L.L., Erisman, J.W., 2011. Nitrogen Processes in the Atmosphere, the European Nitrogen Assessment. Cambridge University Press.

Hudman, R.C., Russell, A.R., Valin, L.C., Cohen, R.C., 2010. Interannual variability in soil nitric oxide emissions over the United States as viewed from space. Atmos. Chem. Phys. 10, 9943—9952. http://dx.doi.org/10.5194/acp-10-9943-2010.

Hudman, R.C., Moore, N.E., Mebust, A.K., Martin, R.V., Russell, A.R., Valin, L.C., Cohen, R.C., 2012. Steps towards a mechanistic model of global soil nitric oxide emissions: implementation and space based-constraints. Atmos. Chem. Phys. 12, 7779—7795. http://dx.doi.org/10.5194/acp-12-7779-2012.

Jaeglé, L., Martin, R.V., Chance, K., Steinberger, L., Kurosu, T.P., Jacob, D.J., Modi, A.I., Yoboué, V., Sigha-Nkamdjou, L., Galy-Lacaux, 2004. C.: satellite mapping of rain-induced nitric oxide emissions from soils. J. Geophys. Res 109 http://dx.doi.org/10.1029/2003JD004406.

Kim, D.G., Vargas, R., Bond-Lamberty, B., Turetsky, M.R., 2012. Effects of soil rewetting and thawing on soil gas fluxes: a review of current literature and suggestions for future research. Biogeosciences 9, 2459—2483.

Laouali, D., Galy-Lacaux, C., Diop, B., Delon, C., Orange, D., Lacaux, J.P., Akpo, A., Lavenu, F., Gardrat, E., Castera, P., 2012. Long term monitoring of the chemical composition of precipitation and wet deposition fluxes over three Sahelian savannas. Atmos. Envirom. 50, 314—327.

Laville, P., Lehuger, S., Loubet, B., Chaumartin, F., Cellier, P., 2011. Effect of management, climate and soil conditions on N 2 O and NO emissions from an arable crop rotation using high temporal resolution measurements. Agric. For. Meteorol. 151, 228—240.

Le Dantec, V., Epron, D., Dufrêne, E., 1999. Soil CO₂ efflux in a beech forest :comparison of two closed dynamic systems. Plant Soil 214 (1—2), 125—132.

Le Roux, X., Abbadie, L., Lensi, R., Serça, D., 1995. Emission of nitrogen monoxide from African tropical ecosystems: control of emission bysoil characteristics in humid and drysavannas of West Africa. J. Geophys. Res. 100, 23133—23142.

Levine, J.S., Winstead, E.L., Parsons, D.A.B., Scholes, M.C., Scholes, R.J., Corer III, W.R., Cahoon Jr., D.R., Sebacher, D.I., 1996. Biogenic soil emissions of nitric oxide (NO) and nitrous oxide (N2O) from savannasin South Africa: the impact of wetting and burning. J. Geophys. Res 101 (D19), 23,689—23,697.

Liu, S., Hu, R., Cai, G., Lin, S., Zhao, J., Li, Y., 2014. The role of UV-B radiation and precipitation on straw decomposition and topsoil C turnover. Soil Biol. Biochem. 77, 197—202.

Livesley, S.J., Grover, S., Hutley, L.B., Jamali, H., Butterbach-Bahl, K., Fest, B., Beringer, J., Arndt, S.K., 2011. Seasonal variation and fire effects on CH₄, N₂O and CO₂ exchange in savanna soils of northern Australia. Agric. For. Meteorol. 151, 1440—1452.

Lloyd, D., Boddy, L., Davies, K.J.P., 1987. Persistence of bacterial denitrification capacity under aerobic conditions" the rule rather than the exception. FEMS Microbiol. Ecol. 45, 185—190.

Loubet, B., Decuq, C., Personne, E., Massad, R.S., Flechard, C., Fanucci, O., Mascher, N., Gueudet, J.-C., Masson, S., Durand, B., Genermont, S., Fauvel, Y., Cellier, P., 2012. Investigating the stomatal, cuticular and soil ammonia fluxes over a growing trital crop under high acidic loads. Biogeosciences 9, 1537—1552.

Ludwig, J., Meixner, F.X., Vogel, B., Forstner, J., 2001. Soil-air exchange of nitric oxide: an overview of processes, environmental factors, and modelling studies. Biogeochemistry 52, 225—257.

Marquina, S., Donoso, L., Pérez, T., Gil, J., Sanhueza, E., 2013. Losses of NO and N2O emissions from Venezuelan and other worldwide tropical N-fertilized soils. J. Geophys. Res. Biogeosciences 118, 1094—1104. http://dx.doi.org/10.1002/jgrg.20081.

Massad, R.-S., Loubet, B., Tuzet, A., Cellier, P., 2008. Relationship between ammonia stomatal compensation point and nitrogen metabolism in arable crops: current status of knowledge and potential modelling approaches. Environ. Pollut. 154 (3), 390—403.

Massad, R.-S., Nemitz, E., Sutton, M.A., 2010. Review and parameterisation of bi-directional ammonia exchange between vegetation and the atmosphere. Atmos. Chem. Phys. 10, 10359—10386. http://dx.doi.org/10.5194/acp-10-10359-2010.

McCalley, C.K., Sparks, J.P., 2008. Controls over nitric oxide and ammonia emissions from Mojave Desert soils. Oecologia 156, 871—881.

Meixner, F.X., Fickinger, Th, Marufu, L., Serça, D., Nathaus, F.J., Makina, E., Mukurumbira, L., Andreae, M.O., 1997. Preliminary results on nitric oxide emission from a southern African savanna ecosystem. Nutr. Cycl. Agroecosyst. 48, 123–138.

Meixner, F.X., Yang, W.X., 2006. In: DÓ doroco, P., Porporato, A. (Eds.), Biogenic Emissions of Nitric Oxide and Ditrous Oxide from Arid and Semi-arid Land, Dryland Ecohydrology. Kluwer Academic Publishers B.V, Dordrecht, The Netherlands, pp. 23–46.

Meijide, A., Dıez, J.A., Sanchez-Martın, L., Lopez-Fernandez, S., Vallejo, A., 2007. Nitrogen oxide emissions from an irrigated maize crop amended with treated pig slurries and composts in a Mediterranean climate. Agr. Ecosyst. Environ. 121, 383–394.

Moorhead, D.L., Reynolds, J.F., 1991. A general model of litter decomposition in the northern Chihuahuan desert. Ecol. Modell. 56, 197–219.

Moyano, F.E., Manzoni, S., Chenu, C., 2013. Responses of soil heterotrophic respiration to moisture availability: an exploration of processes and models. Soil Biol. Biochem. 59, 72–85.

Neftel, A., Blatter, A., Schmid, M., Lehmann, B., Tarakanov, S.V., 2000. An experimental determination of the scale length of N2O in the soil of a grassland. J. Geophys. Res. 105 (D10), 12,095–12,103.

Nemitz, E., Sutton, M.A., Gut, A., San Jose, R., Husted, S., Schjoerring, J.K., 2000. Sources and sinks of ammonia within an oilseed rape canopy. Agr. For. Meteorol. 105, 385–404.

Nemitz, E., Milford, C., Sutton, M.A., 2001. A two-layer canopy compensation point model for describing bi-directional biosphere/atmosphere exchange of ammonia, Q. J. Roy. Meteor. Soc. 127, 815–833.

Ngao, J., Longdoz, B., Perrin, D., Vincent, G., Epron, D., Le Dantec, V., Soudani, K., Aubinet, M., Willm, F., Granier, A., 2006. Cross-calibration functions for soil CO2 efflux measurements systems. Ann. For. Sci. 63, 477–484.

Ni, J.Q., Heber, A.J., Lim, T.T., Diehl, C.A., Duggilara, R.K., Haymore, B.L., Sutton, A.L., 2000. Ammonia emission from a large mechanically-ventilated swine building during warm weather. J. Anv. Qual. 29 (N 3).

Oswald, R., Behrendt, T., Ermel, M., Wu1, D., Su, H., Cheng, Y., Breuninger, C., Moravek, A., Mougin, E., Delon, C., Loubet, B., Pommerening-Röser, A., Sörgel, M., Pöschl, U., Hoffmann, T., Andreae, M.O., Meixner, F.X., Trebs, I., 2013. HONO emissions from soil bacteria as a major source of atmospheric reactive nitrogen. Science 341, 1233. http://dx.doi.org/10.1126/science.1242266.

Pape, L., Ammann, C., Nyfeler-Brunner, A., Spirig, C., Hens, K., Meixner, F.X., 2009. An automated dynamic chamber system for surface exchange measurement of non-reactive and reactive trace gases of grassland ecosystems. Biogeosciences 6, 405–429. http://dx.doi.org/10.5194/bg-6-405-2009.

Parrish, D.D., Fehsenfeld, F.C., 2000. Methods for gas-phase measurements of ozone, ozone precursors and aerosol precursors. Atmos. Environ. 34, 1921–1957.

Parton, W., Silver, W.L., Burke, I.C., Grassens, L., Harmon, M.E., Currie, W., King, J.Y., Adair, E.C., Brandt, L.A., Hart, S.C., Fasth, B., 2007. Global-scale similarities in nitrogen release patterns during long-term decomposition. Sci. New Ser. 315 (No. 5810), 361–364.

Phillips, S.B., Arya, S.P., Aneja, V.P., 2004. Ammonia flux and dry deposition velocity from near-surface concentration gradient measurements over a grass surface in North Carolina. Atmos. Environ. 38, 3469–3480.

Pilegaard, K., 2013. Processes regulating nitric oxide emissions from soils. Phil. Trans. R. Soc. B 2013 (368), 20130126.

Predotova, M., Gebauer, J., Diogo, R.V.C., Schlecht, E., Buerkert, A., 2010. Emissions of ammonia, nitrous oxide and carbon dioxide from urban gardens in Niamey, Niger. Field Crops Res. 115, 1–8.

Pumpanen, J., Kolari, P., Ilvesniemi, H., Minkkinen, K., Vesala, T., Niinistö, S., Lohila, A., Larmola, T., Morero, M., Pihlatie, M., Janssens, I., Curiel Yuste, J., Grünzweig, J.M., Reth, S., Subke, J.-A., Savage, K., Kutsch, W., Østreng, G., Ziegler, W., Anthoni, P., Lindroth, A., Hari, P., 2004. Comparison of different chamber techniques for measuring soil CO2 efflux. Agric. For. Meteorol. 123, 159–176.

Rasmussen, M.O., Gottsche, F.M., Diop, D., Mbow, C., Olesen, F.S., Fensholt, R., Sandholt, I., 2011. Tree survey and allometric models for tiger bush in northern Senegal and comparison with tree parameters derived from high resolution satellite data. Int. J. Appl. Earth Obs. Geoinf. 13, 517–527.

Riedo, M., Milford, C., Schmid, M., Sutton, M.A., 2002. Coupling soil-plant-atmosphere exchange of ammonia with ecosystem functioning in grasslands. Ecol. Model. 158, 83–110.

Robertson, L.A., Kuenen, J.G., 1984. Aerobic denitrification: a controversy revived. Arch. Microbiol. 139, 351–354.

Roelle, P.A., Aneja, V.P., 2002. Characterization of ammonia emissions from soils in the upper coastal plain, North Carolina. Atmos. Environ. 36, 1087–1097.

Rufino, M.C., Brandt, P., Herrero, M., Butterbach-Bahl1, K., 2014. Reducing uncertainty in nitrogen budgets for African livestock systems. Environ. Res. Lett. 9, 105008 (14pp).

Saunders, M.J., Kansiime, F., Jones, M.B., 2012. Agricultural encroachment: implications for carbon sequestration in tropical African wetlands. Glob. Change Biol. 18, 1312–1321. http://dx.doi.org/10.1111/j.1365-2486.2011.02633.x.

Schaeffer, S.M., Billings, S.A., Evans, R.D., 2003. Responses of soil nitrogen dynamics in a Mojave desert ecosystem to manipulations in soil carbon and nitrogen availability. Oecologia 134 (No. 4), 547–553.

Schlesinger, W.H., Reynolds, J.F., Cunningham, G.L., Huenneke, L.F., Jarrell, W.M., Virginia, R.A., Whitford, W.G., 1990. Biological feedbacks in global desertification. Sci. New Ser. 247 (4946), 1043–1046.

Schwinning, S., Sala, O.E., Loik, M.E., Ehleringer, J.R., 2004. Thresholds, memory, and seasonality: understanding pulse dynamics in arid/semi-arid ecosystems. Oecologia 141, 191–193.

Serça, D., Delmas, R., Le Roux, X., Parsons, D.A.B., Scholes, M.C., Abbadie, L., Lensi, R., Ronce, O., Labroue, L., 1998. Comparison of nitrogen monoxide emissions from several African tropical ecosystems and influence of season and fire. Glob. Biogeochem. Cy. 12 (4), 637–651.

Smith, M.S., Tiedje, J.M., 1979. Phases of nitrification following oxygen depletion in soil. Soil Biol. biochem. 11, 261–267.

Steinkamp, J., Ganzeveld, L.N., Wilcke, W., Lawrence, M.G., 2009. Influence of modelled soil biogenic NO emissions on related trace gases and the atmospheric oxidizing efficiency. Atmos. Chem. Phys. 9, 2663–2677. http://dx.doi.org/10.5194/acp-9-2663-2009.

Stewart, D.J., Taylor, C.M., Reeves, C.E., McQuaid, J.B., 2008. Biogenic nitrogen oxide emissions from soils. Impact on NOx and ozone over West Africa during AMMA (african monsoon multidisciplinary analysis): observational study. Atmos. Chem. Phys. 8, 2285–2297.

Sutton, M.A., Asman, W.A.H., Schjoerring, J.K., 1994. Dry deposition of reduced nitrogen. Tellus 46B, 255–273.

Sutton, M.A., Nemitz, E., Erisman, J.W., Beier, C., Butterbach Bahl, K., Cellier, C., de Vries, W., Cotrufo, F., Skiba, U., Di Marco, C., Jones, S., Laville, P., Soussana, J.F., Loubet, B., Twigg, M., Famulari, D., Whitehead, J., Gallagher, M.W., Neftel, A., Flechard, C., Herrmann, B., Calanca, P.L., Schjoerring, J.K., Daemmgen, U., Horvath, L., Tang, Y.S., Emmett, B.A., Tietema, A., Pe nuelas, J., Kesik, M., Brueggemann, N., Pilegaard, K., Vesala, T., Campbell, C.L., Olesen, J.E., Dragosits, U., Theobald, M.R., Levy, P., Mobbs, D.C., Milne, R., Viovy, N., Vuichard, N., Smith, J.U., Smith, P.E., Bergamaschi, P., Fowler, D., Reis, S., 2007. Challenges in quantifying biosphere–atmosphere exchange of nitrogen species. Environ. Pollut. 150, 125–139.

Sutton, M.A., Nemitz, E., Milford, C., Campbell, C., Erisman, J.W., Hensen, A., Cellier, P., David, M., Loubet, B., Personne, E., Schjoerring, J.K., Mattsson, M., Dorsey, J.R., Gallagher, M.W., Horvath, L., Weidinger, T., Meszaros, R., Dammgen, U., Neftel, A., Herrmann, B., Lehman, B.E., Flechard, C., Burkhardt, 2009. J., Dynamics of ammonia exchange with cut grassland: synthesis of results and conclusions of the GRAMINAE integrated experiment. Biogeosciences 6, 2907–2934.

Tagesson, T., Mastepanov, M., Tamstorf, M.P., Eklundh, L., Schubert, P., Ekberg, A., Sigsgaard, C., Christensen, T.R., Ström, L., 2012. High-resolution satellite data reveal an increase in peak growing season gross primary production in a high-Arctic wet tundra ecosystem 1992-2008. Int. J. Appl. Earth Obs. Geoinf. 18, 407–416.

Tagesson, T., Fensholt, R., Cropley, F., Guiro, I., Horion, S., Ehammer, A., Ardö, J., 2015a. Dynamics in carbon exchange fluxes for a grazed semi-arid savanna ecosystem in West Africa. Agric. Ecosyst. Environ. 205, 15–24.

Tagesson, T., Fensholt, R., Guiro, I., Rasmussen, M.O., Huber, S., Mbow, C., Garcia, M., Horion, S., Sandholt, I., Holm-Rasmussen, B., Göttsche, F.M., Ridler, M.-E., Olén, N., Olsen, J.L., Ehammer, A., Madsen, M., Olesen, F.S., Ardö, J., 2015b. Ecosystem properties of semi-arid savanna grassland in West Africa and its relationship to environmental variability. Glob. Change Biol. 21, 250–264.

Traoré, S., Ouattara, K., Ilstedt, U., Schmidt, M., Thiombiano, A., Malmer, A., Nyberg, G., 2015. Effect of land degradation on carbon and nitrogen pools in two soil types of a semi-arid landscape in West Africa. Geoderma 241–242, 330–338.

Turner, M.D., Hiernaux, P., 2015. The effects of management history and landscape position on inter-field variation in soil fertility and millet yields in southwestern Niger. Agric. Ecosyst. Environ. 211, 73–83.

Van Asperen, H., Warneke, T., Sabbatini, S., Nicolini, G., Papale, D., Notholt, J., 2015. The role of photo- and thermal degradation for CO2 and CO fluxes in an arid ecosystem. Biogeosciences 12, 4161–4174.

Wang, L., Manzoni, S., Ravi, D.Riveros-Iregui, S., Caylor, K., 2015. Dynamic interactions of ecohydrological and biogeochemical processes in water-limited systems. Ecosphere 6 (8), 133. http://dx.doi.org/10.1890/ES15-00122.1.

Wentworth, G.R., Murphy, J.G., Gregoire, P.K., Cheyne, C.A.L., Tevlin, A.G., Hems, R., 2014. Soil–atmosphere exchange of ammonia in a non-fertilized grassland: measured emission potentials and inferred fluxes. Biogeosciences 11, 5675–5686.

Wichink Kruit, R.J., van Pul, W.A.J., Otjes, R.P., Hofschreuder, P., Jacobs, A.F.G., Holtslag, A.A.M., 2007. Ammonia fluxes and derived canopy compensation points over non-fertilized agricultural grassland in The Netherlands using the new gradient ammonia – high accuracy – monitor (GRAHAM). Atmos. Environ. 41, 1275–1287.

Xu, X., Tian, H., Hui, D., 2008. Convergence in the relationship of CO2 and N2O exchanges between soil and atmosphere within terrestrial ecosystems. Glob. Change Biol. 14, 1651–1660. http://dx.doi.org/10.1111/j.1365-2486.2008.01595.x.

Yan, X., Ohara, T., Akimoto, H., 2005. Statistical modelling of global soil NOx emissions. Glob. Biogeochem. Cy. 19 http://dx.doi.org/10.1029/2004GB002276. GB3019.

Yienger, J.J., Levy II, H., 1995. Empirical model of global soilbiogenic NOx emissions. J. Geophys. Res. 100, 11447–11464.

Zhang, Y., Liu, J., Mu, Y., Pei, S., Lun, X., Chai, F., 2011. Emissions of nitrous oxide, nitrogen oxides and ammonia from a maize field in the North China plain. Atmos. Environ. 45, 2956–2961.